

Metallicity estimates for A-, F-, and G-type stars from the Edinburgh-Cape blue object survey

T. C. Beers,¹ S. Rossi,² D. O’ Donoghue,³ D. Kilkenney,³ R. S. Stobie,³ C. Koen,³ and R. Wilhelm⁴

¹*Department of Physics & Astronomy, Michigan State University, E. Lansing, MI 48824*

²*Instituto Astronômico e Geofísico, Universidade de São Paulo, Av. Miguel Stefano 4200, 04301-904, São Paulo, Brazil*

³*South African Astronomical Observatory, PO Box 9, Observatory 7935, South Africa*

⁴*McDonald Observatory, University of Texas, Austin, TX 78712*

Accepted 2000 June 30. Received 2000 June 29; in original form 2000 June 28

ABSTRACT

The Edinburgh-Cape Blue Object Survey is an ongoing project to identify and analyse a large sample of hot stars selected initially on the basis of photographic colours (down to a magnitude limit $B \sim 18.0$) over the entire high-Galactic-latitude southern sky, then studied with broadband UBV photometry and medium-resolution spectroscopy. Due to unavoidable errors in the initial candidate selection, stars that are likely metal-deficient dwarfs and giants of the halo and thick-disk populations are inadvertently included, yet are of interest in their own right. In this paper we discuss a total of 206 candidate metal-deficient dwarfs, subgiants, giants, and horizontal-branch stars with photoelectric colours redder than $(B - V)_0 = 0.3$, and with available spectroscopy. Radial velocities, accurate to $\sim 10 - 15 \text{ km s}^{-1}$, are presented for all of these stars. Spectroscopic metallicity estimates for these stars are obtained using a recently recalibrated relation between Ca II K-line strength and $(B - V)_0$ colour. The identification of metal-poor stars from this colour-selection technique is remarkably efficient, and competitive with previous survey methods. An additional sample of 186 EC stars with photoelectric colours in the range $-0.4 \leq (B - V)_0 < 0.3$, comprised primarily of field horizontal-branch stars and other, higher-gravity, A- and B-type stars, is also analysed. Estimates of the physical parameters T_{eff} , $\log g$, and $[\text{Fe}/\text{H}]$ are obtained for cooler members of this subsample, and a number of candidate RR Lyrae variables are identified.

Key words: Surveys – Galaxy: halo — Galaxy: thick disk — Galaxy: abundances — Stars: Population II.

1 INTRODUCTION

Deep, and in particular, *complete* surveys of stars in the halo of the Galaxy always turn up objects of astrophysical interest outside of the original targets of the survey. The Edinburgh-Cape Blue Object Survey (hereafter, EC survey) is no different in this respect (see Stobie et al. 1997 for a detailed description). Briefly, the EC survey is intended to discover large numbers of stars in the southern sky with colours normally associated with the blue stellar populations of the Galaxy, such as white dwarfs and subdwarf O- and B-type stars, in a similar fashion to the Palomar-Green survey in the northern hemisphere (Green, Schmidt, & Liebert 1986). The initial colour-selection criterion for EC stars makes use of a $B, U - B$ polygon in the (photographic) magnitude-colour diagram (see Fig. 2 of Stobie et al. 1997). The attempt was made, on a plate-by-plate basis, to set the red boundaries of

this polygon in such a way as to exclude most of the F- and G-type stars, while retaining most of the bluer objects. The shape of the boundary differs from plate to plate, and naturally becomes somewhat less clear at fainter magnitudes, due to the increasing errors in the photographic photometry. For the EC survey, a contamination level of ~ 20 per cent in the original selection was deemed acceptable. During the course of spectroscopic and photometric follow-up observations of the EC stars brighter than $B \sim 16.5$, it has become clear that many of these ‘contaminant’ stars are in fact of great interest as probes of the metal-poor stellar populations of the Galaxy. The present paper explores the nature of these stars.

In this paper we report radial velocities, stellar classifications, and spectroscopic abundance estimates, expressed in terms of $[\text{Fe}/\text{H}]$, for 321 main-sequence turnoff (TO), sub-

giant (SG), giant (G), and field horizontal-branch (FHB) or other A-type stars identified in the process of the EC survey follow-up campaign. Radial velocities (only) are reported for 73 stars which are likely B-type horizontal-branch (HBB) stars. We note that the present sample contains 108 stars with radial velocity and abundance determinations in the Galactic anti-rotation direction at lower Galactic latitudes ($|b| \leq 45^\circ$); these data provide valuable information concerning the rotation of the halo and thick-disk components of the Galaxy (see, e.g., Chiba & Beers 2000).

2 OBSERVATIONS AND DATA REDUCTION

Broadband *UBV* measurements of EC survey stars have been previously obtained with photoelectric photometers on the SAAO 0.75m and 1.0m telescopes. The majority of the stars in the present paper have had apparent magnitudes and colours reported in Kilkenny et al. (1997) – these have been supplemented with some newer data. Column (1) of Table 1 lists the EC number of the stars in the present sample. The 37 stars in this sample that exhibit possible peculiarities of one kind or another are identified with superscripts attached to their names. Columns (2) and (3) list the equinox 1950.0 coordinates for each star. Errors in these positions are typically ± 2 arcsec. Columns (4) and (5) are the Galactic longitude and latitude, respectively. Columns (6)–(8) report the *UBV* photometry. Stobie et al. (1997) show that the typical errors in the EC photoelectric photometry vary from 0.02 to 0.04 mag as one progresses from the brighter ($V < 13.5$) to the faintest stars ($V > 16.5$). Reddening estimates in the direction toward each star are obtained by interpolation of the Burstein & Heiles (1982) maps. An initial reddening estimate is made assuming the star under consideration lies completely above or below the Galactic dust layer (taken here to have a scale height of $h = 125$ pc). The reddening to a given star at distance D (where available) is reduced compared to the total reddening by a factor $[1 - \exp(-|D \sin b|/h)]$, where b is the Galactic latitude. This estimate, which accuracy typically not better than 0.03 mag, is listed in column (9). For stars that we are unable to assign distances to, we simply adopt the unaltered reddening estimate from Burstein & Heiles.

Medium-resolution ($\sim 3.5 \text{ \AA}$ over two pixels) spectra of EC survey stars were obtained with the RPCS spectrograph (using an intensified Reticon photon counting detector + grating # 6) on the SAAO 1.9m telescope, over the spectral range $3600 \text{ \AA} \leq \lambda \leq 5200 \text{ \AA}$, and with a typical signal-to-noise $10/1 \leq S/N \leq 15/1$. Data reduction was performed using the SAAO program SKIP; a detailed description of the procedures can be found in Stobie et al. (1997).

F- and G-type stars are readily recognized from the spectra based on the strengths of the Ca II H and K lines, centered on $\lambda \sim 3950 \text{ \AA}$, and the CH G-band feature at $\lambda \sim 4300 \text{ \AA}$. Other objects among our program stars appear to be FHB- or A-type stars, based on the depth and breadth of their Balmer lines and the occasional presence of HeI absorption features. Sample spectra of the stars analysed in this paper are shown in Fig. 9 of Stobie et al. (1997).

Fig. 1a shows a histogram of the distribution of apparent V magnitudes for our program stars. Roughly 60 per cent of the EC stars in the present sample are fainter than about

$V = 14.5$, which, for main sequence luminosities or greater, puts them at distances farther than 750 pc away, well outside the thin disk, and approaching the scale height of the thick disk (in the vertical directions). It follows that this sample may contain a substantial fraction of metal-deficient stars. Fig. 1b shows the distribution of de-reddened $(B - V)_0$ colours. It is essentially bi-modal in appearance, with the great majority of the bluer stars being identified below as likely HBB stars.

Fig. 2 is the de-reddened two-colour diagram for the program stars, shown with a solar-abundance main-sequence line from Johnson (1966) superposed. One can clearly recognize dwarfs of low metal abundance that, due to the de-blanking effect, lie above the main-sequence solar-metallicity line. In addition, there are a number of metal-poor FHB stars that lie close to this line due to the effect of low surface gravity on their colours. A handful of stars with colours we would associate with the Blue Metal-Poor (BMP) stars of Preston, Beers, & Shectman (1994) are present as well, with $0.0 \leq (B - V)_0 \leq 0.35$ and $-0.5 \leq (U - B)_0 \leq -0.1$. The grouping of stars with colours in the range $-0.4 \leq (B - V)_0 \leq 0.0$ and $-1.0 \leq (U - B)_0 \leq -0.1$ are dominated by horizontal-branch B-type (HBB) stars, but may additionally include main-sequence and subdwarf B-type stars.

A number of stars in our program sample have been identified by previous surveys. Table 2 lists these identifications, obtained by conducting a search of the SIMBAD database for stars with coordinates (and commensurate colours or spectral types) within 1 arcmin of the positions listed in Table 1.

3 DERIVED PARAMETERS

3.1 Radial velocities and line indices

Radial velocities are obtained for each of our program stars using the line-by-line and cross-correlation techniques, described in detail in Beers et al. (1999), and references therein. Application of these techniques to the slightly higher-resolution spectra of the HK survey follow-up effort (1-2 \AA) yielded velocities accurate to on the order of 7–10 km s^{-1} , so we expect that our present results should only be slightly worse than this, on the order of ~ 10 –15 km s^{-1} . This level of accuracy is still sufficient to be useful for analysis of the kinematics for the thick-disk and halo populations, since their velocity dispersions are in the range ~ 45 –150 km s^{-1} . Measurements of the heliocentric radial velocities, after correction for the Earth's rotation and orbital motion, are listed in column (10) of Table 1.

For each star, the derived (geocentric) radial velocities are used to place a set of fixed bands for the derivation of line-strength indices, which are pseudo-equivalent widths of prominent spectral features. The bands we employ are summarized in Table 3. A complete discussion of the choice of bands, and the ‘band-switching’ scheme used to produce our derived Ca II K-line index, KP, and Balmer-line index, HP2, is provided in Beers et al. (1999).

Line indices (in \AA) for each of the program stars are reported in columns (11)–(14) of Table 1. Column (12) lists He I line indices (at wavelengths $\lambda = 4026 \text{ \AA}$ and $\lambda = 4471$

Å), where available, with the blue and the red line listed in the left and right sides of the column, respectively. In order for a line-index measurement to be considered a detection, we require that the derived indices reach a minimum value of 0.25 \AA . The He I indices (and the G-band index GP) are useful in the detection of likely ‘composite stars’ – stars that exhibit a combination of spectra and colours that indicate the possible presence of a companion star of different spectral type than the classification we have adopted (see Fig. 3 of Kilkenny et al. 1997 for other examples from the EC survey).

3.2 Stellar classifications

Stellar classifications, based on visual inspection of the spectra, and consideration of the observed UBV photometry, are provided in column (15) of Table 1. For the majority of the program stars, these classifications are the same as those given in Kilkenny et al. (1997). However, a number of stars in the present sample did not appear in the previously published list, hence classifications for these stars are shown here for the first time.

For the purpose of further analysis it is convenient to divide the sample according to colour. We first consider the subsample of stars satisfying $-0.4 \leq (B - V)_0 \leq 0.4$, and refer to these stars below as the ‘hot-star’ subsample. Stars with colours $(B - V)_0 \geq 0.3$ are considered ‘cool stars.’ The overlap of these two samples in the range $0.3 \leq (B - V)_0 \leq 0.4$ is used to provide a check on the abundance determinations obtained from two different calibrations. Although the calibrations were constrained by comparison with very different stellar samples, the two calibrations do share a common model-atmosphere source, hence they are not totally independent of one another.

3.3 The horizontal-branch B-type stars

There are 73 stars among our program sample that are likely to be hot horizontal-branch B-type (HBB) stars; these are listed in Table 4. For stars at such high temperatures it is not feasible to obtain estimates of physical parameters based on analysis of medium-resolution spectra. It is possible that some of the stars listed in Table 4 are *not* HBB stars at all (alternatives would include sdB, as well as post-AGB stars – see discussions in Hambly et al. 1997 and Kendall et al. 1997), but we have no means of making further refinements in their classifications based on the present data. A discussion of their radial velocity distribution is presented in §4 below.

There are four stars in Table 4 that fall in the colour range $0.0 \leq (B - V)_0 \leq 0.4$ and $(U - B)_0 \leq 0.4$ that may be composite stars – these are identified in the table with a colon (:) following their names.

3.4 Physical parameter estimates for the hot stars

Wilhelm, Beers, & Gray (1999a) discuss the development and calibration of a spectroscopic and photometric technique which enables the identification and classification of FHB- and other A-type stars over the temperature range

$6000 \leq T_{\text{eff}} \leq 10000 \text{ K}$. This technique makes use of broadband UBV colours predicted from model atmosphere calculations, Balmer-line profiles, Ca II K equivalent widths, and a synthetic-template comparison method, to estimate the physical parameters T_{eff} , $\log g$, and $[\text{Fe}/\text{H}]$, with precision on the order of $\sigma(T_{\text{eff}}) = \pm 250 \text{ K}$, $\sigma(\log g) = \pm 0.25 \text{ dex}$, and $\sigma([\text{Fe}/\text{H}]) = \pm 0.3 \text{ dex}$, respectively. Wilhelm et al. (1999b) apply this methodology to a large sample of hot stars identified in the HK objective-prism survey, and discuss some of the advantages and pitfalls of this approach. As part of their high-resolution follow-up study of BMPs, Preston & Sneider (2000) have confirmed that the abundances for BMPs derived by Wilhelm et al. (1999b) are well-matched with those obtained from their own analysis, giving additional confidence in the estimates of metallicity obtained by these methods. In §3.7 below, we discuss an ‘internal’ comparison of abundance determination for stars in the overlapping colour regions of the hot and cool subsamples.

Table 5 summarizes the results obtained by application of the Wilhelm et al. (1999a) technique to the hot-star subsample. Column (1) lists the EC star name. Columns (2) and (3) list estimates of effective temperature and surface gravity, respectively. Note that for stars with colours at or near the blue limits of the Wilhelm et al. grids of model atmospheres ($(B - V)_0 = -0.25$ and/or $(U - B)_0 = -0.45$), the estimated temperatures and surface gravities may be subject to larger errors. These stars are indicated with an appended colon following the estimated parameter.

Columns (4) and (5) of Table 5 list estimates of metal abundance obtained from analysis of the Ca II K line. The metallicity estimate $[\text{Fe}/\text{H}]_{\text{WK}}$ is based on the measured equivalent width of the Ca II K line. The estimate $[\text{Fe}/\text{H}]_{\text{CTA}}$ is obtained from profile fits to this same line. For the lower signal-to-noise spectra of some program stars, these estimates occasionally differ markedly – this is especially true for the hotter stars with very weak Ca II K lines. Column (6) lists estimates of abundance, $[\text{Fe}/\text{H}]_{\text{MTA}}$, obtained by comparison of two ‘metallic-line regions,’ falling in the wavelength intervals $4175 \text{ \AA} \leq \lambda \leq 4310 \text{ \AA}$ and $4360 \text{ \AA} \leq \lambda \leq 4500 \text{ \AA}$, with template synthetic spectra. Following the precepts of Wilhelm et al., we adopt an abundance estimate $[\text{Fe}/\text{H}]_{\text{AVG}}$, listed in column (7), that is the mean of the two most-consistent estimators from columns (4)-(6). Column (8) lists the absolute difference in the abundance determinations from the most-consistent estimators from one another. It should be kept in mind that the lowest abundance that can be reliably obtained for stars in the hot-star subsample is $[\text{Fe}/\text{H}] = -3.0$. Again, in the case of stars with colours at or near the grid limits of the models, a colon is appended to their estimated abundances to indicate additional uncertainty.

Column (9) of Table 5 lists the stellar type classifications obtained from application of the Wilhelm et al. methods. Four classes are used: FHB – a likely field-horizontal branch star; A – a star with main-sequence gravity typical of A-type stars, BMPs, and other, slightly cooler, early F-type stars; FHB/A – an indeterminate classification, and Am – a star with apparently main-sequence gravity and a large discrepancy between the metallic-line-region abundance estimate and those estimates based on the Ca II K line, a phenomenon often associated with Am (and Ap) stars (see Wilhelm et al. 1999a, 1999b for more details). For the stars

in Table 5 classified as Am, the appropriate abundance estimate is that listed in column (6), $[\text{Fe}/\text{H}]_{\text{MTA}}$.

Column (12) of Table 5 identifies a number of stars with the entry ‘r’ that exhibit discrepancies between their Balmer-line strengths and their observed broadband colours, which might arise from spectroscopic and photometric observations of an RR Lyrae variable taken ‘out of phase.’ These identifications are tentative, and should be confirmed on the basis of further photometric follow-up. Note that several stars in this table are known RR Lyrae variables (indicated with an ‘R’ in column (12)).

There are 21 stars in Table 5 that are identified in Table 1 as having possible peculiarities in their spectra and/or colours, leading to somewhat less confidence in the proper assignment of their spectral classifications and in the derived estimates of their physical parameters. These stars are indicated in Table 5 with an appended colon following their adopted class in column (9). A colon has also been appended to their physical parameter estimates listed in the table.

3.5 Distance estimates for the hot stars

For the stars in Table 5 classified as FHB, estimates of absolute magnitude and distance (in parsecs) are derived following the procedure described by Wilhelm et al. (1999b), and are listed in Columns (10) and (11), respectively. For stars classified as A or Am, we have adopted an estimate of distance, calibrated by the main sequences of young open clusters (shifted appropriately to account for their metal abundances), as described by Beers et al. (2000). This methodology differs from that used by Wilhelm et al., and produces distance estimates for these stars that are as much as a factor of two *less* than those authors report for stars of the same classification (note that the previous procedure did not explicitly take metallicity into account, producing much of the discrepancy). No estimated distances are given for the stars classified as FHB/A.

3.6 Abundance determinations for the cool stars

Beers et al. (1999) describe a technique for the estimation of $[\text{Fe}/\text{H}]$ from medium-resolution spectroscopy of stars, based on the strength of the Ca II K line as a function of dereddened $(B - V)_0$ colour, with accuracy on the level of 0.15–0.2 dex over the abundance range $-4.0 \leq [\text{Fe}/\text{H}] \leq 0.0$. The EC spectra are not generally of sufficiently high signal-to-noise to make use of the Auto-Correlation Function technique described by Beers et al., however, we can still make use of their correction matrices to ensure that, in particular, the more metal-rich cool stars do not have their abundances significantly *under*-estimated by the Ca II K-line technique.

We have employed this methodology to obtain abundance estimates for the 206 cool EC stars with available spectra and colours redder than $(B - V)_0 = 0.3$. The results of the abundance analysis are summarized in Table 6. Column (1) lists the EC star. Column (2) lists the type classification obtained from the precepts described in Beers et al. (1999), with the caveat described below. The Beers et al. classification scheme is based on a comparison of the derived dereddened colour with the expected location of a star in the colour-magnitude diagram for stars of a variety of ages

(from 5 to 15 Gyrs) and metallicities ($-3.0 \leq [\text{Fe}/\text{H}] \leq 0.0$) obtained from the Revised Yale Isochrones (Green 1988; King, Demarque, & Green 1988). Column (3) lists the estimated absolute magnitude, M_V , and column (4) lists the associated distance estimate (in parsecs). In cases where the type classification is ambiguous, e.g., TO/FHB or FHB/TO, alternative absolute magnitudes and distances are provided in parentheses. Column (5) lists the estimated metallicity obtained by application of the Beers et al. calibration, $[\text{Fe}/\text{H}]_{\text{K3}}$, and its associated one-sigma error. For the 12 cool stars noted in Table 1 with peculiarities, we have attached a colon to their type classifications and metallicity estimates.

The caveat in the type classifications mentioned above concerns our separation of FHB and TO stars in the colour range $0.3 \leq (B - V)_0 \leq 0.5$, which differs from that used previously in the HK survey follow-up. The original classification scheme (dating back to Beers, Preston, & Shectman 1985) was designed for application to stars of very low metallicity ($[\text{Fe}/\text{H}] < -2.0$). However, since we are now obtaining abundance estimates for stars with metallicities up to the solar value, the procedure by which the ‘split’ between FHB and TO stars has to be modified. In the original scheme, stars in the colour range $0.3 \leq (B - V)_0 \leq 0.5$, which includes both FHB and TO stars, were assigned classifications based on the simple criteria:

$$\text{TO} : \quad (U - B)_0 \leq -0.1$$

$$\text{FHB} : \quad (U - B)_0 > -0.1$$

This split is not adequate for stars with abundances $[\text{Fe}/\text{H}] > -2.0$.

Fig. 3 shows the ‘limiting’ $(U - B)_0$ colours as a function of metallicity, as predicted from the Revised Yale Isochrones for (a) stars with surface gravities $\log g \leq 3.0$ (appropriate for FHB stars in this colour range—see Wilhelm et al. 1999a) and (b) stars with $\log g \geq 4.0$ (appropriate for TO stars in this colour range). For the present classification exercise, we make the FHB/TO assignments by comparison with these limiting lines (broadened slightly to include estimated reddening errors in $(U - B)_0$ on the order of 0.02 mag). Stars with $(U - B)_0$ colours *above* the TO line (i.e., at lower values of $(U - B)_0$) are classified as TO, while those *below* the FHB line (i.e., at higher values of $(U - B)_0$) are classified as FHB. Stars of intermediate surface gravities fall between the lines, and their classifications are less certain, but we assign a class based on the closest of the two limiting lines. In most cases accurate photometry should produce a reliable assignment. For stars with ambiguous classifications, we have attached a colon to the abundance determination listed in Table 6 to indicate the additional uncertainty in this estimate.

3.7 Comparison of abundance determinations

There are 26 stars in the colour region $0.3 \leq (B - V)_0 \leq 0.4$ that appear in both the hot- and cool-star subsamples discussed above, and hence have metallicity estimates determined from two different calibrations. Fig. 4 shows a comparison of these estimates. The agreement between the two metallicity estimates is generally good, with a slight tendency for the more metal-deficient stars determined from

the hot-star calibration to have derived abundances that are higher than those determined from the cool-star calibration. The difference between these estimates, in the sense $[\text{Fe}/\text{H}]_{\text{AVG}} - [\text{Fe}/\text{H}]_{\text{K3}}$, as quantified by the biweight estimate of central location discussed by Beers, Flynn, & Gebhardt (1990), is $C_{BI} = +0.1$ dex. The biweight scale of their difference is $S_{BI} = 0.5$ dex, only slightly higher than the expected error obtained from the square root of the quadratic sum of the errors of the methods, approximately 0.4 dex.

4 RADIAL VELOCITY DISTRIBUTIONS FOR THE EC STARS

Fig. 5 displays histograms of the heliocentric radial velocities for the three subsamples of EC stars considered in this paper. The distributions are quite similar to one another, and all exhibit dispersions consistent with stars selected from the Galactic halo population, $\sigma_{\text{los}} \sim 100 - 120 \text{ km s}^{-1}$. The appearance of the cool-star subsample distribution suggests the presence of a low-dispersion population, which is likely to include members of the metal-weak thick disk of the Galaxy – note that Chiba & Beers (2000) have shown the metal-weak thick disk extends to metallicities as low as $[\text{Fe}/\text{H}] = -2.0$. The hot-star distribution appears to have little or no evidence for the presence of this low-dispersion population – a result of the generally larger distances explored by this subsample as compared to the cool-star subsample. Fig. 6 shows a comparison of the cumulative distributions of these two subsamples as a function of height above the Galactic plane. Over half (~ 65 per cent) of the cool-star subsample is located within 1 kpc of the plane, the region most likely to be dominated by metal-weak thick-disk stars, while only ~ 25 per cent of the hot-star subsample is located this close to the plane.

Fig. 7 displays the distribution of heliocentric radial velocities for the cool-star and hot-star subsamples as a function of estimated $[\text{Fe}/\text{H}]$. The high-velocity stars from these subsamples are clearly drawn from similar (likely, identical) parent populations, while the presence of a low-dispersion population of metal-weak stars down to $[\text{Fe}/\text{H}] \sim -2.0$ is clear among the cool-star subsample.

5 EFFICIENCY OF THE EC SURVEY FOR DETECTION OF VERY METAL-POOR STARS

Figs. 8a and 8b show the distribution of derived metal abundances for the hot-star and cool-star subsamples, respectively. Figs. 9a and 9b are the cumulative distributions for these same data sets, which we compare below to the results of other surveys for metal-poor stars.

A variety of techniques have been used previously to discover metal-poor stars in the Galaxy. The approaches can be broadly divided into two categories – proper-motion-selected stars, such as those discussed by Ryan & Norris (1991) and Carney et al. (1994), and objective-prism surveys, such as the HK survey described by Beers, Preston, & Shectman (1992). Inspection of the cumulative metallicity distribution of the EC stars in the cool-star subsample, shown in Fig. 9a, suggests that the discovery efficiency of

stars with abundances less than $[\text{Fe}/\text{H}] = -1.0$ is significantly better than that obtained from spectroscopic follow-up of proper-motion-selected stars shown in Fig. 9c. The cumulative distribution function of metallicity for the HK-survey stars, shown in Fig. 9d, appears to be superior for the identification of large numbers of stars with $[\text{Fe}/\text{H}] \leq -1.0$, but since it was targeted at such stars this is perhaps not a great surprise. Applying the definition of the ‘effective yield’ (EY) of survey techniques for extremely metal-poor stars described by Beers (2000) (numbers of stars discovered with $[\text{Fe}/\text{H}] \leq -2.0$ compared to the number of stars inspected), the relevant numbers for the samples shown in Figs. 8a-d are: EY (EC cool stars) = 0.19, EY (EC hot stars) = 0.18, EY (proper-motion-selected stars) = 0.11, EY (objective-prism-selected stars) = 0.50.

We wish to emphasize that the EYs of the EC stars quoted above is made based on the *entire* set of stars examined in this paper. Clearly, if our purpose was simply to select the most likely metal-poor candidates, the *UBV* photometry obtained during the course of the EC follow-up would allow us to substantially increase the EY of this technique. For instance, if we were to restrict the colours to only include stars in the range $0.3 \leq (B-V)_0 \leq 0.5$, the EY of the EC survey would rise dramatically, to on the order of 0.30. If one further restricted the stars of interest in this colour range to include only stars with $(U-B)_0 \leq -0.1$, the EY of the EC survey would rise to 0.40. This result bodes well for future colour-selected samples of metal-poor candidates, such as those obtained from the Sloan Digital Sky Survey (e.g., Lenz et al. 1993). Christlieb & Beers (2000) describe a refined selection technique based on automated classification of prism spectra from the Hamburg/ESO Objective-Prism Survey that achieves EY = 0.80 for metal-deficient dwarfs near the halo main-sequence turnoff *without* the need for a photometric pre-filter.

One might wonder whether the relatively high EY of the EC survey could result because, at faint apparent magnitudes, one is exploring deep enough into the halo population of the Galaxy that a random sample of stars might be expected to contain a large fraction of metal-deficient objects. That is, how much has the (original, photographic) colour selection actually helped with the identification of truly metal-poor stars? One way to empirically address this question is by making a comparison of the metallicity distribution function (MDF) of the cool stars obtained at different distances above or below the Galactic plane. Figs. 10a and 10b are comparisons of the low-abundance tail of the MDF for the subset of stars with $|Z| \leq 1000$ pc with that for the subset of stars with $|Z| > 1000$ pc. Only the low-abundance tails have been compared to avoid complications introduced by the presence of the metal-weak thick disk. As can be seen in the Figures, although there does exist a slight tendency for the more distant stars to include objects of greater metal deficiency, it is not a particularly strong one, and may be influenced by the small number statistics. Furthermore, Reid & Majewski (1993) have shown that in order to obtain a ‘pure’ sample of halo stars (without contamination from the tail of the substantially more populous thick-disk component) one must reach out to distances greater than $\sim 5 - 7$ kpc above or below the Galactic plane. For stars near the main-sequence turnoff, which dominate the EC cool-star subsample, this would correspond to apparent

magnitudes as faint as $V \sim 18.5$, substantially fainter than the limiting magnitude of the stars for which photometry and spectroscopy have been obtained during the EC survey follow-up.

Of particular interest are the 36 stars in the cool-star subsample with $[\text{Fe}/\text{H}] \leq -2.0$; the lowest-metallicity cool star has an abundance $[\text{Fe}/\text{H}] = -2.94$. The hot-star subsample includes another 20 stars with $[\text{Fe}/\text{H}] \leq -2.0$. Stars of such low metallicity are quite rare in the Galaxy, at least brighter than the apparent magnitude limits that have been explored to date.

We expect that spectroscopic observations of additional stars from the EC survey that satisfy the colour criteria described herein, but which at present do not have spectroscopic data, will result in the discovery of additional stars with $[\text{Fe}/\text{H}] \leq -2.0$. Based on the results found to date, as the EC survey progresses, we might expect the discovery of another ~ 250 stars with $[\text{Fe}/\text{H}] \leq -2.0$, for a total of ~ 300 stars with abundance less than 1 per cent of solar, and a total of ~ 1250 stars with $[\text{Fe}/\text{H}] \leq -1.0$. By way of comparison, the total yield of stars with $[\text{Fe}/\text{H}] \leq -1.0$ in the HK survey follow-up to date numbers ~ 2000 stars. Hence, a dedicated campaign to obtain medium-resolution spectroscopy of the EC ‘contaminants’ can make a substantial contribution to the database of known metal-deficient stars in the Galaxy.

ACKNOWLEDGEMENTS

TCB acknowledges support for this work from grant AST 95-29454 from the National Science Foundation. SR acknowledges partial support for this work from grant 200068/95-4 CNPq, Brazil, and from the Brazilian Agency FAPESP. We also thank a semi-anonymous referee for comments and suggestions which improved the presentation.

This work made use of the SIMBAD database, operated at CDS, Strasbourg, France.

REFERENCES

- Beers, T.C. 2000, in A. Weiss, T. Abel, & V. Hill, eds, *The First Stars*, Proceedings of the Second MPA/ESO Workshop, Springer, Berlin, p. 3.
- Beers, T.C., Preston, G.W., & Shectman, S.A. 1985, *AJ*, 90, 2089
- Beers, T.C., Flynn, K., & Gebhardt, K. 1990, *AJ*, 100, 32
- Beers, T.C., Preston, G.W., & Shectman, S.A. 1992, *AJ*, 103, 1987
- Beers, T.C., Rossi, S., Norris, J.E., Ryan, S.G., & Shefler, T. 1999, *AJ*, 117, 981
- Beers, T.C., Chiba, M., Yoshii, Y., Platais, I., Hanson, R.B., Fuchs, B., & Rossi, S. 2000, *AJ*, 119, 2866
- Burstein, D., & Heiles, C. 1982, *AJ*, 87, 1165
- Carney, B.W., Laird, J., Latham, D.W., & Aguilar, L. 1994, *AJ*, 107, 2290
- Chiba, M., & Beers, T.C. 2000, *AJ*, 119, 2843
- Christlieb, N., & Beers, T.C., in M. Takada-Hidai & H. Ando, eds, *Subaru HDS Workshop on Stars and Galaxies: Decipherment of Cosmic History with Spectroscopy*, NAO, Mitaka, p. 255
- Green, E.M. 1988, in A.G.D. Philip, ed, *Calibration of Stellar Ages*, L. Davis Press, Schenectady, p. 81
- Green, R.F., Schmidt, M., & Liebert 1986, *ApJS*, 61, 305
- Hambly, N.C., Rolleston, W.R.J., Keenan, F.P., Dufton, P.L., & Saffer, R.A. 1997, *ApJS*, 111, 419
- Johnson, H.L. 1966, *ARA&A*, 4, p. 193
- Kendall, T.R., Dufton, P.L., Keenan, F.P., Beers, T.C., & Hambly, N.C. 1997, *A&A*, 317, 82
- Kilkenny, D., O’Donoghue, D., Koen, C., Stobie, R.S., & Chen, A. 1997, *MNRAS*, 287, 867
- King, C.C., Demarque, P., & Green, E.M. 1988, A.G.D. Philip, ed, *Calibration of Stellar Ages*, L. Davis Press, Schenectady, p. 211
- Lenz, D.D., Newberg, J., Rosner, R., Richards, G.T., & Stoughton, C., *ApJS*, 119, 121
- Preston, G.W., & Sneden, C. 2000, *AJ*, in press
- Preston, G.W., Beers, T.C., & Shectman, S.A. 1994, *AJ*, 108, 538
- Reid, N., & Majewski, S.R. 1993, *ApJ*, 409, 635
- Ryan, S.G., & Norris, J.E. 1991, *AJ*, 101, 1865
- Stobie, R.S. et al. 1997, *MNRAS*, 287, 848
- Wilhelm, R., Beers, T.C., & Gray, R.O. 1999a, *AJ*, 117, 2308
- Wilhelm, R., Beers, T.C., Sommer-Larsen, T.C., Pier, J.R., Layden, A.C., Flynn, C., Rossi, S., & Christensen, P.-R. 1999b, *AJ*, 117, 2329.

FIGURE CAPTIONS

Figure 1. (a) Distribution of photoelectric V magnitudes for the EC survey stars considered herein. (b) Distribution of photoelectric de-reddened $(B - V)_0$ colours for the EC survey stars.

Figure 2. De-reddened two-colour diagram for the EC survey stars. The line shown is a solar-abundance main-sequence gravity line taken from Johnson (1966). The crosses correspond to stars noted in Table 1 with some peculiarities (binary, possible variable, composite) associated with them. Errors in the photometry (on the order of 0.02 mag) are too small to be usefully shown on the scale of this plot.

Figure 3. Limiting $(U - B)_0$ colours of stars in the colour range $0.3 \leq (B - V)_0 \leq 0.5$, as a function of metallicity, obtained from the Revised Yale Isochrones. The region above the solid line corresponds to the locations of stars with surface gravities typical of main-sequence TO stars, while the region below the dashed line applies for stars with surface gravities of FHB stars. See text for additional explanation.

Figure 4. Comparison of abundances estimated for EC survey stars in the colour range $0.3 \leq (B - V)_0 \leq 0.4$ determined using the techniques of Wilhelm et al. (1999a), $[\text{Fe}/\text{H}]_{\text{AVG}}$, with those determined using the techniques of Beers et al. (1999), $[\text{Fe}/\text{H}]_{\text{K3}}$. The solid line is the one-to-one line. The dashed line is a locally weighted regression line. The agreement between the two techniques is good down to $[\text{Fe}/\text{H}] \sim -2.0$. Below this abundance, the Wilhelm et al. technique appears to slightly overestimate the derived abundance as compared to the cool-star calibration.

Figure 5. Radial velocities for the three subsamples of EC survey stars – (a) the EC cool stars, (b) the EC hot stars, and (c) the EC HBB stars. In each case, the solid line indicates the best-fit (single) Gaussian distribution.

Figure 6. Cumulative distribution functions for the EC cool-star (filled circles) and hot-star (open circles) subsamples, respectively, as a function of absolute distance from the Galactic plane. Note that the cool-star subsample contains a large fraction of stars with distances less than 1 kpc from the plane, while only a minor fraction of the hot-star subsample lies this close.

Figure 7. Radial velocities as a function of estimated metallicity for the EC cool stars (filled circles) and the EC hot stars (open circles). Note that both distributions are quite similar. The cool stars, in addition to a halo component, appear to include a low velocity-dispersion population of stars over the metallicity interval $-2.0 \leq [\text{Fe}/\text{H}] \leq 0.0$, most likely associated with the metal-weak thick disk.

Figure 8. Histograms of the estimated abundances for (a) the EC hot stars, and (b) the EC cool stars.

Figure 9. Cumulative distribution functions of metallicity for stars selected by various survey techniques – (a) the EC cool stars, (b) the EC hot stars, (c) high-proper-motion stars

from Carney et al. (1994), and (d) HK survey stars, selected by the objective-prism technique.

Figure 10. Comparison of the metallicity distribution functions for two subsets of the cool-star subsample with $[\text{Fe}/\text{H}] \leq -2.0$. (a) A histogram of the two distributions. The dashed histogram is for stars with distances in excess of 1 kpc from the plane, while the solid histogram is for stars closer than 1 kpc. Note that, with the exception of a single bin at low abundance, the histograms are quite similar to one another. (b) Cumulative distribution functions of the two distributions. The open circles connected by the dashed line are for those stars with distances in excess of 1 kpc from the plane, while the filled circles connected by the solid line are for those stars closer than 1 kpc. Note that the cumulative distributions are quite similar to one another.

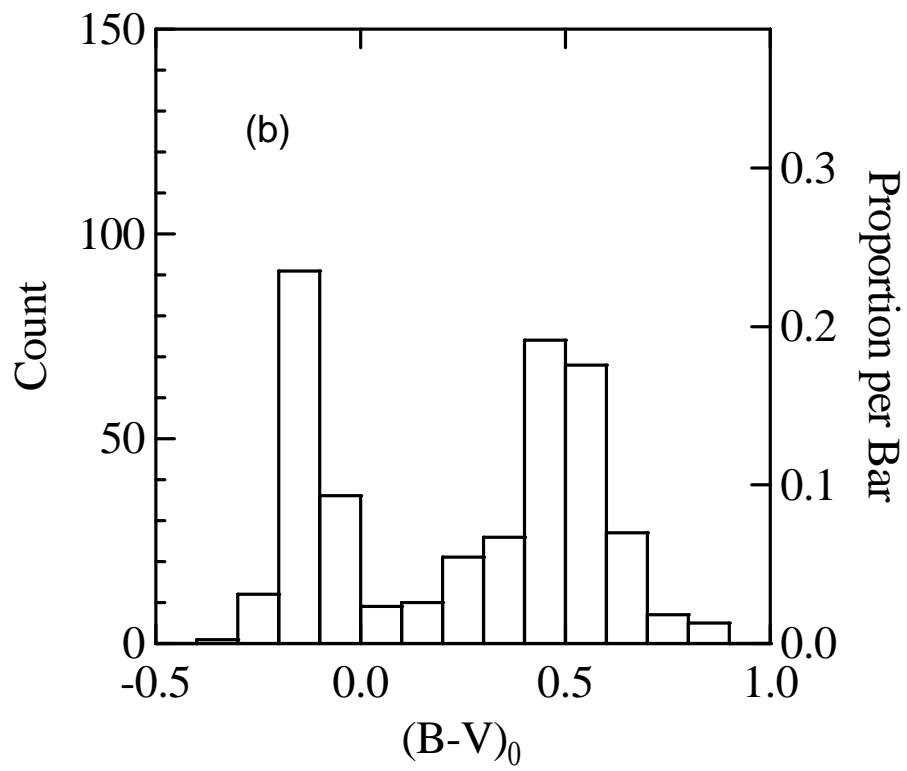
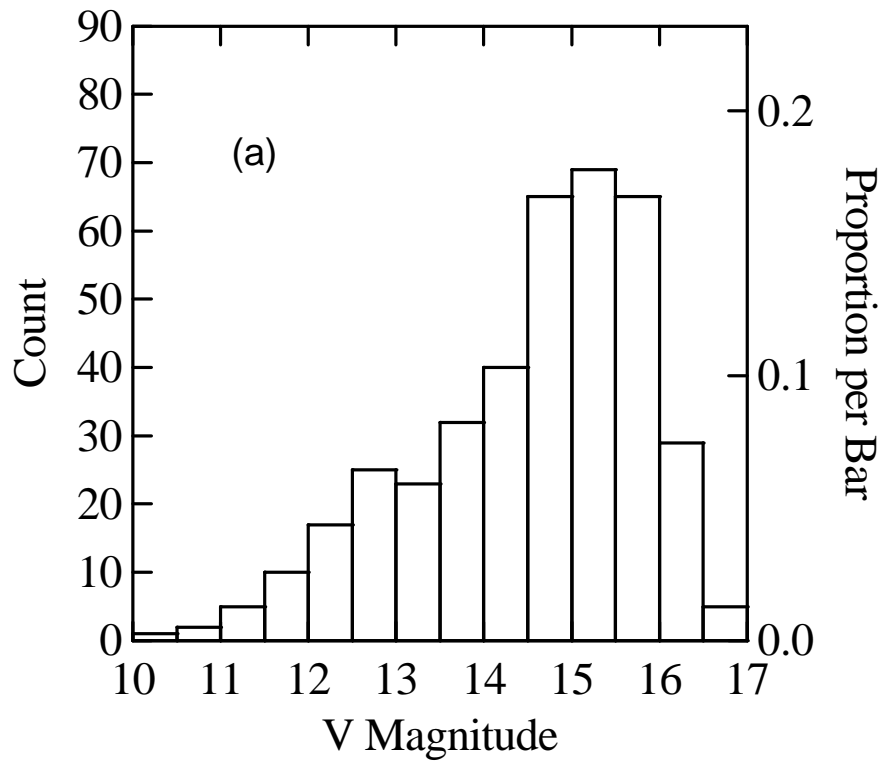


TABLE 1. Observed quantities for EC program stars

Star (1)	RA (1950) (2)	DEC (3)	l (4)	b (5)	V (6)	$B - V$ (7)	$U - B$ (8)	E_{B-V} (9)	VEL (10)	KP (11)	HeI (12)	HP2 (13)	GP (14)	EC Class (15)
00097–3243	00 09 43.0	–32 43 50	358.5	–80.0	16.38	0.39	0.17	0.00	58	1.76	... , ...	4.17	...	F?
00179–6503 ^e	00 17 59.1	–65 03 06	308.3	–52.0	14.36	0.00	–0.42	0.00	71	...	0.62 , 0.66	8.86	0.92	~B7/HBB
00230–2340	00 23 05.1	–23 40 45	64.0	–83.1	14.09	0.59	0.05	0.01	–7	9.03	... , ...	1.96	4.14	G
00237–2317	00 23 43.8	–23 17 13	67.4	–83.0	14.57	–0.13	–0.54	0.02	112 , 0.25	7.60	...	HBB
00269–5602	00 26 55.2	–56 02 24	309.4	–61.1	13.81	–0.14	–0.59	0.00	157	...	0.42 , 0.80	7.17	...	HBB
00316–2543	00 31 41.2	–25 43 45	55.4	–85.8	14.88	0.50	–0.06	0.01	–15	8.18	... , ...	3.61	2.67	~F5
00341–7725	00 34 07.4	–77 25 53	304.1	–39.9	13.50	0.54	–0.09	0.06	–36	7.34	... , ...	2.62	2.76	~F5
00347–7711	00 34 44.0	–77 11 28	304.0	–40.2	14.54	0.54	–0.06	0.06	–68	7.15	... , ...	1.69	3.53	~F7
00381–1423	00 38 09.1	–14 23 07	111.5	–76.7	14.48	–0.06	–0.43	0.01	–65	...	0.32 , 0.42	7.41	0.46	HBB?/B?
00448–6351	00 44 51.0	–63 51 12	303.8	–53.5	14.02	0.61	–0.09	0.00	88	8.22	0.38 , ...	2.84	5.47	G
00538–8121 ^a	00 53 50.2	–81 21 00	302.8	–36.0	15.14	0.28	–0.55	0.08	–110	4.17	0.35 , 0.31	4.54	1.16	~F2
00594–6309	00 59 28.6	–63 09 50	301.0	–54.2	12.24	0.49	–0.07	0.00	39	7.15	... , ...	3.72	2.53	~F5
01021–6222	01 02 10.0	–62 22 28	300.3	–55.0	14.62	0.65	0.01	0.00	65	8.96	... , ...	1.86	5.12	G
01030–5232	01 03 04.0	–52 32 30	298.0	–64.7	15.53	0.44	–0.06	0.00	144	3.72	0.28 , 0.73	4.63	1.50	A–F
01181–7826	01 18 10.5	–78 26 49	301.1	–38.8	13.66	0.52	–0.10	0.06	–53	6.41	0.70 , ...	4.79	2.81	~F5
01218–5735	01 21 51.2	–57 35 00	294.4	–59.3	13.90	0.67	0.08	0.00	37	7.78	... , ...	0.97	5.17	G
01218–5741	01 21 49.2	–57 41 28	294.4	–59.2	12.35	0.64	0.07	0.00	30	8.08	... , ...	1.13	4.13	G
01226–6746	01 22 37.2	–67 46 25	298.1	–49.3	13.64	0.52	0.01	0.00	23	7.64	... , 0.25	3.09	3.81	~F6
01233–2807	01 23 19.1	–28 07 43	220.5	–82.4	14.77	0.83	0.49	0.01	37	10.73	... , ...	0.82	5.07	K
01327–6630	01 32 45.0	–66 30 36	296.2	–50.3	14.59	0.47	–0.16	0.00	49	5.00	... , 0.52	3.57	1.26	~F4
01497–6658	01 49 44.3	–66 58 17	294.0	–49.4	13.40	0.45	–0.10	0.00	32	6.38	... , ...	3.89	1.79	~F4
01510–3919	01 51 03.1	–39 19 03	259.7	–72.4	14.29	–0.19	–0.80	0.00	–48	...	0.64 , 0.67	6.24	...	HBB/B4
02023–7847	02 02 18.5	–78 47 10	298.6	–38.0	14.19	0.49	–0.17	0.07	228	1.88	... , ...	4.72	0.49	~F2
02133–5827	02 13 23.6	–58 27 19	283.5	–55.6	15.74	0.83	0.49	0.00	–30	8.12	0.28 , 0.50	1.05	5.78	F–G
02317–2144	02 31 46.0	–21 44 32	205.0	–66.0	15.07	0.52	–0.02	0.01	80	8.20	... , 0.56	3.64	4.00	F–G
02368–1725	02 36 51.7	–17 25 29	196.8	–63.2	15.38	0.47	–0.21	0.01	–16	3.37	... , 0.34	3.40	1.23	F?
02518–6611	02 51 53.2	–66 11 40	285.5	–46.8	16.15	–0.15	–0.54	0.01	204 , 0.32	6.68	...	HBB
02536–3218	02 53 41.7	–32 18 33	231.0	–62.6	14.64	0.64	–0.10	0.00	66	9.30	... , 0.42	1.06	5.25	F–G
03148–4056	03 14 49.8	–40 56 16	246.9	–57.2	16.13	0.43	–0.24	0.00	271	1.43	... , 0.98	5.87	1.41	F–G
03224–3558	03 22 25.5	–35 58 05	237.5	–56.5	12.72	0.56	–0.03	0.00	8	5.66	... , 0.41	3.78	3.43	~F6
03240–6229	03 24 05.2	–62 29 27	278.1	–46.7	11.12	–0.09	–0.31	0.01	–15	...	0.41 , 0.59	8.44	0.35	B7/HBB
03289–0304	03 28 55.2	–03 04 05	187.6	–44.7	8.91	0.42	–0.05	0.01	22	6.58	... , 0.31	4.19	1.86	~F2
03330–7735	03 33 01.4	–77 35 14	292.9	–36.4	14.94	0.68	0.11	0.08	0	7.66	... , ...	0.29	6.83	G
03436–4748	03 43 36.8	–47 48 13	256.1	–50.6	14.24	–0.19	–0.65	0.00	61	...	0.45 , ...	6.57	...	~B5/HBB
03462–5813	03 46 16.9	–58 13 47	270.7	–46.5	9.94	–0.12	–0.47	0.00	59	...	0.29 , 1.01	7.60	...	~B6/HBB
03495–7850	03 49 35.5	–78 50 58	293.4	–34.9	15.89	–0.13	–0.66	0.09	432 , 0.36	7.25	0.31	HBB
03528–3734	03 52 49.6	–37 34 06	239.8	–50.3	13.79	0.42	–0.22	0.00	179	3.25	0.42 , ...	4.06	1.30	~F2
03546–3737	03 54 39.7	–37 37 10	239.9	–50.0	12.78	0.54	–0.01	0.00	41	8.33	... , ...	2.90	4.48	G
03547–3738	03 54 43.4	–37 38 28	239.9	–50.0	13.63	0.51	–0.03	0.00	16	7.56	... , ...	3.89	2.91	~F5
03569–3728	03 56 54.7	–37 28 48	239.6	–49.5	11.57	0.51	–0.04	0.00	63	7.95	... , ...	3.39	2.91	~F5

TABLE 1. (continued)

Star (1)	RA (1950) (2)	DEC (3)	l (4)	b (5)	V (6)	$B - V$ (7)	$U - B$ (8)	E_{B-V} (9)	VEL (10)	KP (11)	HeI (12)	HP2 (13)	GP (14)	EC Class (15)
03572-3729	03 57 17.3	-37 29 21	239.7	-49.5	12.99	0.28	0.02	0.00	21	4.40	0.42 , ...	7.67	1.04	~A8
03597-3727	03 59 43.7	-37 27 48	239.6	-49.0	12.68	0.44	-0.09	0.00	119	7.55	... , ...	4.80	2.49	~F2
03598-3742	03 59 52.7	-37 42 16	240.0	-48.9	12.78	0.53	0.05	0.00	79	8.55	... , ...	3.89	3.82	~F8
03599-3723	03 59 59.4	-37 23 02	239.5	-48.9	13.54	0.60	-0.07	0.00	89	9.35	... , ...	1.22	4.44	G
04005-3742	04 00 35.0	-37 42 48	240.0	-48.8	12.96	0.48	-0.05	0.00	53	7.99	... , 0.64	3.16	3.26	~F4
04009-3721	04 00 59.0	-37 21 02	239.4	-48.7	12.81	0.50	-0.02	0.00	27	7.36	... , 0.27	2.55	3.04	F5
04013-3746	04 01 20.6	-37 46 49	240.1	-48.6	11.38	0.58	0.08	0.00	65	8.90	... , ...	3.18	4.28	~F8
04026-3726	04 02 37.4	-37 26 06	239.6	-48.4	12.42	0.62	0.08	0.00	-13	8.75	... , ...	1.65	4.37	G
04040-8518	04 04 04.3	-85 18 23	298.9	-30.4	15.17	0.84	0.52	0.14	-72	9.17	... , ...	0.90	4.61	G
04224-5424	04 22 27.8	-54 24 09	263.3	-43.0	14.95	-0.10	-0.54	0.00	99	0.36	0.32 , ...	6.68	...	HBB
04300-5341	04 30 01.2	-53 41 48	262.0	-42.1	13.66	-0.17	-0.59	0.00	150	...	0.45 , 0.41	7.17	...	HBB
04359-2745	04 35 57.3	-27 45 34	227.4	-40.2	14.61	0.56	0.17	0.00	-13	8.95	0.77 , ...	1.37	4.23	~F8
04420-1908	04 42 04.5	-19 08 12	217.4	-36.3	13.14	-0.07	-0.49	0.01	208	...	0.53 , 0.50	5.11	0.32	~B6/HBB
04460-3215 ^e	04 46 04.4	-32 15 08	233.7	-39.0	11.66	0.05	-0.44	0.00	-6	1.12	... , ...	8.12	0.63	~A3/HBA
04571-3729	04 57 08.6	-37 29 50	240.8	-37.6	14.36	0.49	-0.06	0.00	34	7.95	... , ...	4.05	3.92	late F ₁ e?
04573-1506	04 57 20.2	-15 06 54	214.6	-31.4	15.37	0.47	0.00	0.04	55	5.85	... , 1.40	3.37	4.10	F-G
04578-3749	04 57 51.5	-37 49 35	241.2	-37.5	14.99	0.44	-0.20	0.00	252	4.86	0.27 , ...	1.95	0.80	~F2
04580-3726	04 58 03.8	-37 26 48	240.8	-37.4	14.80	0.56	-0.09	0.00	29	8.82	... , ...	1.76	3.74	~F8
05002-1314	05 00 13.4	-13 14 31	212.9	-30.0	13.91	0.59	-0.12	0.05	33	6.94	... , 0.32	2.87	2.42	F
05024-7723	05 02 29.8	-77 23 25	289.6	-32.4	14.89	0.64	-0.01	0.11	117	7.97	1.19 , ...	5.01	2.69	F?
05028-7725	05 02 52.9	-77 25 49	289.7	-32.4	13.48	0.56	-0.01	0.11	2	8.12	... , ...	4.73	2.60	~F5
05039-3423	05 03 54.1	-34 23 09	237.2	-35.7	14.67	0.55	-0.03	0.00	108	8.26	... , ...	2.52	3.75	F
05053-3342	05 05 21.3	-33 42 18	236.5	-35.3	14.82	0.51	-0.20	0.00	296	6.96	... , 0.85	1.93	2.73	~F5
05063-2330	05 06 19.3	-23 30 28	224.7	-32.4	14.01	1.35	0.03	0.01	125	7.06	... , 0.29	0.43	3.98	K
05067-7720	05 06 45.8	-77 20 35	289.5	-32.2	15.29	0.66	0.22	0.11	27	10.12	... , ...	1.48	3.63	G
05070-2725	05 07 05.8	-27 25 57	229.2	-33.4	13.36	0.48	-0.06	0.00	50	7.18	... , ...	4.33	2.32	~F2
05077-6225	05 07 45.3	-62 25 01	272.0	-35.7	14.53	-0.12	-0.49	0.00	147 , ...	7.45	...	HBA
05084-2919	05 08 27.1	-29 19 55	231.5	-33.7	13.48	-0.09	-0.40	0.00	98	...	0.56 , 0.41	8.26	...	HBB
05094-3103	05 09 24.9	-31 03 23	233.6	-33.9	12.85	0.52	-0.09	0.00	117	6.22	... , ...	2.04	2.77	~F8
05098-3047	05 09 48.3	-30 47 30	233.3	-33.7	14.83	0.58	-0.05	0.00	97	9.11	... , 0.63	1.39	4.19	~F8
05101-3607	05 10 09.9	-36 07 19	239.6	-34.8	14.74	0.52	-0.17	0.01	284	6.27	... , 0.52	3.30	1.75	F
05107-7724	05 10 44.1	-77 24 04	289.5	-32.0	16.20	-0.04	-0.48	0.11	111	0.31	0.67 , 0.87	6.90	...	HBB
05116-3357	05 11 41.9	-33 57 22	237.1	-34.1	14.78	0.52	-0.08	0.01	33	7.11	... , ...	3.95	2.56	~F5
05117-3559	05 11 47.1	-35 59 02	239.5	-34.5	14.44	0.49	-0.22	0.01	197	5.36	... , ...	3.23	1.83	F
05121-7726	05 12 07.9	-77 26 09	289.5	-31.9	15.62	0.66	-0.07	0.11	227	6.10	... , ...	5.10	...	G
05131-6050	05 13 07.5	-60 50 31	269.9	-35.3	15.96	-0.10	-0.48	0.00	251	...	0.63 , 0.88	5.17	...	~B5e/HBB
05138-5914	05 13 52.1	-59 14 52	268.0	-35.3	15.55	-0.13	-0.69	0.00	338	...	0.60 , 0.97	4.23	...	~B3/HBB?
05190-3512	05 19 01.2	-35 12 25	239.0	-32.9	13.15	-0.10	-0.53	0.02	166	0.36	0.88 , 1.46	6.90	0.28	HBB
05198-4005	05 19 51.9	-40 05 13	244.8	-33.6	15.73	-0.12	-0.49	0.00	60	0.55	0.43 , ...	7.11	...	HBB
05331-4234	05 33 07.5	-42 34 04	248.1	-31.6	15.17	0.50	-0.09	0.01	-5	6.62	... , 0.35	3.25	2.00	~F5

TABLE 1. (continued)

Star (1)	RA (1950) (2)	DEC (3)	l (4)	b (5)	V (6)	$B - V$ (7)	$U - B$ (8)	E_{B-V} (9)	VEL (10)	KP (11)	HeI (12)	HP2 (13)	GP (14)	EC Class (15)
05344-5747	05 34 29.8	-57 47 32	266.1	-32.7	13.83	0.57	-0.04	0.04	-50	7.88	0.35 , 0.81	2.93	3.81	~F8
05377-5834	05 37 47.3	-58 34 00	267.0	-32.3	14.65	0.58	-0.10	0.04	143	4.52	... , ...	1.25	2.02	~F8
05438-4741	05 43 49.6	-47 41 00	254.4	-30.5	12.64	-0.07	-0.42	0.07	79	0.38	0.31 , 0.39	7.45	...	~B6/HBB
05515-6231	05 51 35.0	-62 31 40	271.7	-30.7	9.28	-0.10	-0.48	0.04	-10	...	0.42 , 0.34	6.62	...	~B6/HBB
05581-5856	05 58 06.9	-58 56 33	267.6	-29.7	15.29	-0.16	-0.90	0.05	321	0.42	0.95 , 1.58	3.63	...	~B2/HBB
05581-6201	05 58 06.5	-62 01 57	271.2	-29.9	15.91	-0.11	-0.46	0.04	320	0.46	... , 1.01	6.54	...	HBB
05587-5808	05 58 47.1	-58 08 55	266.7	-29.5	15.08	0.31	-0.20	0.05	96	0.91	... , 0.35	6.66	1.26	HBA?
06012-7810	06 01 14.4	-78 10 27	289.7	-29.2	13.26	-0.08	-0.70	0.11	65	0.27	0.98 , 0.80	3.33	...	HBB/B3
06031-7744 ^e	06 03 09.1	-77 44 02	289.2	-29.2	14.43	0.26	-0.40	0.11	-51	1.92	... , 0.36	5.32	0.98	HBA?
06250-7842	06 25 00.8	-78 42 11	290.3	-28.0	15.01	0.53	-0.15	0.15	106	1.75	1.13 , ...	1.96	1.64	F?
06353-7725	06 35 20.0	-77 25 15	288.8	-27.4	13.29	0.50	-0.04	0.15	-16	6.27	... , ...	4.40	1.47	~F2
06360-7721	06 36 05.7	-77 21 23	288.8	-27.4	15.17	0.59	0.07	0.18	81	9.16	... , ...	1.93	3.37	F/G
09076-1141	09 07 41.2	-11 41 41	241.4	+23.7	16.44	-0.12	-0.67	0.03	177	0.74	... , ...	6.26	...	HBB/B6
09088-1116	09 08 51.0	-11 16 00	241.3	+24.1	15.10	-0.08	-0.46	0.03	182	0.36	... , 0.41	8.16	...	B6/HBB
09120-1155	09 12 00.2	-11 55 40	242.4	+24.4	15.76	-0.15	-0.37	0.04	274	...	1.04 , ...	8.06	0.46	HBB
09222-1243	09 22 16.3	-12 43 25	244.8	+25.8	11.46	0.57	-0.09	0.02	208	7.94	... , ...	1.83	3.47	F7
09227-1245	09 22 47.7	-12 45 15	244.9	+25.9	13.62	0.56	-0.06	0.03	23	7.97	... , ...	2.95	3.23	F7
09278-1246	09 27 53.0	-12 46 39	245.8	+26.8	15.35	0.52	-0.05	0.04	203	8.20	0.77 , 0.85	1.61	2.73	F7
09288-1234	09 28 50.0	-12 34 09	245.8	+27.2	15.41	0.65	0.02	0.04	84	7.00	0.45 , ...	1.64	3.92	G
09290-1650 ^e	09 29 05.8	-16 50 03	249.4	+24.4	16.50	0.40	-0.40	0.05	123 , 0.78	7.97	0.84	HBB
09306-1222	09 30 37.7	-12 22 52	245.9	+27.6	15.52	0.48	-0.26	0.04	248	4.84	0.43 , ...	3.07	1.22	F Pec
09340-1725	09 34 05.1	-17 25 48	250.8	+24.9	14.29	0.72	0.23	0.07	64	8.47	... , ...	1.39	5.00	G
09423-0936	09 42 23.6	-09 36 31	245.7	+31.6	14.85	0.71	0.16	0.03	95	9.39	0.76 , ...	1.64	5.35	early G
09433-1526	09 43 19.1	-15 26 01	250.8	+27.9	15.81	-0.08	-0.57	0.05	245	...	0.80 , 0.53	5.80	0.67	HBB
09479-0931 ^e	09 47 55.5	-09 31 29	246.6	+32.7	14.69	0.32	-0.39	0.03	98	3.42	... , ...	5.46	1.93	F5
09490-1611	09 49 03.6	-16 11 29	252.5	+28.3	15.12	0.49	0.03	0.05	3	3.75	... , ...	5.74	0.84	F0
09550-1554	09 55 05.6	-15 54 43	253.5	+29.6	14.76	0.48	-0.23	0.04	203	3.30	... , 0.32	3.74	0.63	F2
09555-1208	09 55 33.6	-12 08 07	250.4	+32.3	15.01	0.59	0.00	0.03	34	6.31	... , ...	1.93	3.57	G0
09561-1334	09 56 06.6	-13 34 06	251.7	+31.4	15.56	0.50	-0.20	0.05	157	4.09	... , ...	4.61	1.08	F
10008-0749	10 00 50.5	-07 49 44	247.7	+36.2	15.26	0.32	-0.28	0.04	22	3.14	... , ...	5.36	1.58	F5
10087-1227	10 08 45.6	-12 27 54	253.4	+34.3	14.25	0.52	0.08	0.05	58	8.04	... , ...	1.82	3.30	F7
10115-2144	10 11 33.5	-21 44 04	261.2	+27.9	14.41	0.59	0.08	0.05	53	8.61	... , 0.71	1.71	4.23	F8
10153-1731	10 15 19.5	-17 31 26	258.9	+31.7	15.46	-0.06	-0.50	0.07	352	...	0.67 , 0.73	6.64	...	HBB
10163-1238	10 16 22.2	-12 38 51	255.2	+35.5	13.42	0.56	0.04	0.08	13	9.14	... , 0.27	3.37	3.71	F7
10165-1232	10 16 32.6	-12 32 15	255.2	+35.6	13.63	-0.06	-0.41	0.08	67	0.36	... , 0.41	5.87	0.39	A1
10185-0947	10 18 32.5	-09 47 43	253.3	+37.9	15.96	0.43	-0.23	0.04	116	2.27	... , ...	1.93	...	F2
10195-1740	10 19 35.6	-17 40 15	259.9	+32.2	14.61	0.50	-0.07	0.06	28	7.01	0.78 , 1.19	1.54	2.42	G
10197-1231	10 19 47.6	-12 31 09	255.9	+36.1	14.19	0.23	-0.33	0.09	34	2.00	... , 0.29	6.50	1.18	A6
10213-1737	10 21 22.9	-17 37 35	260.3	+32.5	11.43	0.56	-0.02	0.04	-24	8.41	... , ...	2.87	3.64	F8
10221-1929	10 22 09.0	-19 29 53	261.8	+31.2	12.21	-0.08	-0.39	0.07	82	0.43	0.31 , 0.70	6.71	...	HBB/B6

TABLE 1. (continued)

Star (1)	RA (1950) (2)	DEC (3)	l (4)	b (5)	V (6)	$B - V$ (7)	$U - B$ (8)	E_{B-V} (9)	VEL (10)	KP (11)	HeI (12)	HP2 (13)	GP (14)	EC Class (15)
10269–2548	10 26 56.2	–25 48 08	267.1	+26.8	14.54	0.48	–0.27	0.00	209	3.54	… , …	1.78	1.25	F4
10275–1547	10 27 35.5	–15 47 55	260.3	+34.9	12.25	–0.01	–0.31	0.09	35	…	… , …	7.01	0.25	HBB
10289–0951	10 28 54.0	–09 51 08	255.8	+39.6	12.01	0.52	0.02	0.02	16	7.84	… , …	3.77	2.74	F6
10291–2653	10 29 11.6	–26 53 53	268.3	+26.2	13.62	–0.07	–0.42	0.05	107	0.45	… , 0.46	6.33	…	HBB
10292–0957	10 29 17.9	–09 57 33	256.0	+39.6	13.69	0.40	0.01	0.03	64	5.63	… , …	6.37	1.92	F3
10298–2231	10 29 53.3	–22 31 35	265.6	+29.8	15.93	0.42	–0.35	0.06	89	4.13	… , 1.31	3.18	1.68	F
10299–1555	10 29 56.3	–15 55 25	260.9	+35.1	12.43	–0.04	–0.34	0.07	49	0.29	0.34 , 0.53	8.05	0.45	B7/HBB
10381–2731	10 38 10.9	–27 31 55	270.6	+26.7	15.95	0.42	–0.18	0.00	110	1.97	… , 0.49	2.44	…	F0
10391–2043	10 39 06.1	–20 43 28	266.4	+32.5	13.94	0.56	–0.16	0.03	240	7.28	0.50 , …	1.88	2.16	F5
10393–2105	10 39 18.3	–21 05 13	266.7	+32.3	12.82	0.47	–0.04	0.03	–9	7.28	… , …	5.15	2.98	F4
10405–1648	10 40 34.0	–16 48 16	264.1	+35.9	15.84	0.65	–0.12	0.03	64	8.23	… , 1.43	2.55	4.38	F8
10419–1959	10 41 57.8	–19 59 26	266.6	+33.5	12.04	0.59	0.03	0.02	45	7.73	… , …	3.22	4.12	F8
10435–2140	10 43 30.2	–21 40 59	268.1	+32.3	14.60	0.63	0.01	0.04	–27	8.44	0.39 , 0.43	1.79	4.58	F9
10471–2455	10 47 08.9	–24 55 02	270.9	+30.0	14.24	0.56	–0.26	0.09	119	2.63	0.63 , 0.25	3.58	2.57	F8
10496–2452	10 49 40.7	–24 52 46	271.5	+30.3	14.25	0.68	0.09	0.09	–23	8.11	0.46 , 0.80	1.61	4.12	G1
10548–1451	10 54 50.6	–14 51 11	266.2	+39.5	13.73	0.27	0.23	0.04	29	1.11	… , …	9.51	1.36	A2
10548–2724	10 54 52.3	–27 24 16	274.1	+28.7	11.82	0.71	0.13	0.05	45	8.99	… , …	0.99	5.63	G3
10568–2257	10 56 51.2	–22 57 35	272.0	+32.8	15.29	0.31	0.11	0.06	118	2.00	… , 0.32	6.54	1.13	A5
10582–2256	10 58 16.0	–22 56 21	272.3	+33.0	13.77	0.52	0.03	0.06	–11	7.84	… , …	4.02	3.19	F6
10588–1632 ^e	10 58 51.2	–16 32 03	268.5	+38.6	13.60	0.35	–0.38	0.03	74	4.77	0.27 , 0.28	4.28	2.17	F5
11006–2213	11 00 37.5	–22 13 07	272.5	+33.9	16.42	0.23	0.04	0.05	21	3.10	… , 0.49	4.23	…	A–F
11013–2547	11 01 21.7	–25 47 29	274.7	+30.8	15.03	0.39	0.08	0.05	108	2.67	… , 0.59	3.64	1.15	HBA
11024–3246	11 02 25.1	–32 46 02	278.5	+24.7	15.98	0.03	–0.25	0.08	158	0.46	… , …	7.13	0.81	HBA
11033–2344	11 03 21.8	–23 44 12	274.0	+32.9	15.43	0.49	0.06	0.06	345	1.97	… , …	6.85	0.36	HBA
11034–1758	11 03 24.2	–17 58 36	270.6	+37.9	12.48	–0.04	–0.20	0.04	36	0.43	0.55 , …	8.76	…	HBA
11057–2051	11 05 46.6	–20 51 24	273.0	+35.7	14.24	0.65	0.07	0.03	60	10.15	… , 0.36	0.95	4.33	G
11063–2349	11 06 18.2	–23 49 33	274.8	+33.1	15.19	0.52	–0.06	0.07	48	4.62	… , …	4.96	…	early F
11082–2831	11 08 17.5	–28 31 58	277.7	+29.1	13.66	0.84	0.41	0.08	–17	9.81	… , 0.36	1.23	6.05	G7
11084–2607	11 08 26.1	–26 07 21	276.5	+31.3	14.98	0.47	0.04	0.06	102	4.89	… , 0.48	4.13	1.48	F2
11092–2933	11 09 15.1	–29 33 31	278.4	+28.2	14.71	0.60	0.08	0.08	41	7.06	… , …	2.21	3.29	G
11100–1813	11 10 01.5	–18 13 39	272.5	+38.5	6.08	–0.01	–0.09	0.01	25	0.78	… , …	10.01	…	A0
11107–3237	11 10 45.5	–32 37 45	280.2	+25.6	12.44	0.51	–0.02	0.08	–31	6.72	… , …	4.05	3.08	F5
11109–1514	11 10 57.2	–15 14 56	270.9	+41.2	15.24	0.46	–0.16	0.05	76	1.50	0.53 , 0.84	5.17	0.63	A4
11138–1507	11 13 49.1	–15 07 09	271.6	+41.6	15.24	0.54	–0.16	0.04	118	3.07	… , 0.38	1.78	1.62	F4
11163–1635	11 16 20.3	–16 35 45	273.2	+40.6	15.60	0.56	0.05	0.05	27	6.79	0.25 , 0.71	4.61	5.10	G
11183–2731	11 18 19.4	–27 31 10	279.5	+30.9	15.90	0.45	–0.13	0.06	133	3.91	… , …	3.05	0.56	early F
11196–3155	11 19 36.2	–31 55 46	281.8	+27.0	12.60	0.15	–0.30	0.08	24	1.67	… , …	8.53	1.06	A2
11221–2844	11 22 11.2	–28 44 18	281.0	+30.1	14.21	0.23	0.12	0.07	271	0.92	0.81 , 0.41	8.58	0.77	A1
11222–2606	11 22 14.4	–26 06 50	279.8	+32.6	15.23	–0.06	–0.34	0.06	90	…	… , …	7.60	…	HBB
11249–1723	11 24 56.7	–17 23 47	276.1	+40.8	15.70	0.70	0.12	0.03	68	10.19	0.38 , …	1.25	4.31	G

TABLE 1. (continued)

Star (1)	RA (1950) (2)	DEC (3)	l (4)	b (5)	V (6)	$B - V$ (7)	$U - B$ (8)	E_{B-V} (9)	VEL (10)	KP (11)	HeI (12)	HP2 (13)	GP (14)	EC Class (15)
11267–3200	11 26 45.5	–32 00 00	283.4	+27.5	14.65	0.76	0.11	0.07	–43	8.62	... , ...	0.42	4.65	G7
11337–3043	11 33 46.7	–30 43 08	284.5	+29.2	13.12	–0.08	–0.45	0.07	138	0.39	... , 0.25	6.93	0.27	HBB
11340–1830	11 34 03.7	–18 30 50	279.3	+40.6	15.96	0.61	–0.28	0.03	106	3.29	... , ...	0.28	1.71	F–G
11344–2713	11 34 29.7	–27 13 39	283.3	+32.5	16.87	–0.21	–0.69	0.07	216	...	0.63 , ...	6.73	...	HBB
11348–2735 ^b	11 34 50.2	–27 35 57	283.6	+32.2	15.42	0.44	0.22	0.08	18	4.73	... , 0.34	5.59	1.60	F5
11362–2157 ^b	11 36 13.1	–21 57 18	281.6	+37.6	16.32	0.84	0.67	0.03	7	7.81	2.13 , ...	0.88	5.53	G
11366–3217	11 36 38.2	–32 17 34	285.7	+27.9	15.87	–0.14	–0.43	0.07	158	...	0.85 , 0.28	8.43	...	HBB
11372–2938	11 37 17.9	–29 38 07	284.9	+30.4	12.55	–0.12	–0.41	0.05	–11 , ...	7.21	...	HBB
11374–2223	11 37 26.8	–22 23 55	282.1	+37.3	12.80	0.49	0.00	0.03	9	7.03	... , 0.48	3.08	2.66	F5
11405–1807	11 40 34.0	–18 07 00	281.1	+41.6	15.20	0.55	–0.15	0.02	100	4.63	... , ...	1.79	1.85	G
11413–1838	11 41 21.4	–18 38 58	281.5	+41.1	15.66	0.60	–0.11	0.02	82	10.44	... , ...	3.60	5.22	early G
11417–2110	11 41 46.4	–21 10 42	282.8	+38.8	12.80	–0.11	–0.45	0.03	26	0.31	0.81 , 0.66	6.65	...	HBB
11471–3219	11 47 09.6	–32 19 48	288.2	+28.5	12.35	0.43	–0.18	0.07	187	2.91	... , ...	3.71	0.46	F0
11475–2259	11 47 33.8	–22 59 32	285.1	+37.5	14.84	–0.10	–0.54	0.05	49	0.49	... , 0.50	6.24	...	HBB
12000–1549	12 00 00.4	–15 49 50	286.2	+45.2	15.25	0.24	0.17	0.02	44	1.68	... , ...	8.47	0.46	HBA
12021–1744	12 02 09.5	–17 44 41	287.6	+43.4	16.18	0.44	–0.24	0.03	125	4.24	0.90 , 1.23	4.41	1.36	F4
12037–2710	12 03 45.8	–27 10 03	290.8	+34.4	15.82	0.55	–0.17	0.09	7	3.19	... , 0.55	2.28	2.53	F3
12040–3226 ^e	12 04 02.4	–32 26 02	292.1	+29.2	15.77	0.38	–0.57	0.10	93	3.74	0.41 , ...	2.74	2.31	F5
12225–1928	12 22 31.7	–19 28 30	294.5	+42.7	15.98	–0.09	–0.45	0.02	194	0.88	... , 0.29	6.52	...	HBB
12226–2211	12 22 36.0	–22 11 22	295.0	+40.0	15.99	0.67	0.39	0.05	58	10.72	0.85 , 0.94	1.99	5.91	G
12238–1855	12 23 52.7	–18 55 26	294.8	+43.3	14.50	0.85	0.44	0.02	58	10.42	... , ...	2.00	6.03	G5
12256–2707 ^e	12 25 36.5	–27 07 32	296.6	+35.2	16.55	0.13	–0.44	0.07	30	2.76	0.84 , 0.29	5.14	...	F0
12258–1353	12 25 49.8	–13 53 15	294.5	+48.3	15.84	–0.08	–0.49	0.03	245	0.41	0.41 , 0.57	6.61	...	HBB
12266–1557	12 26 36.9	–15 57 25	295.2	+46.3	14.44	0.33	–0.03	0.01	4	4.86	... , 0.69	5.22	1.78	F5
12270–3205 ^b	12 27 03.3	–32 05 45	297.6	+30.3	15.30	0.21	0.18	0.09	128	1.06	... , ...	9.37	...	HBA
12272–1657	12 27 16.5	–16 57 35	295.6	+45.3	12.60	0.47	0.00	0.01	38	5.63	... , ...	4.80	2.39	F5
12288–1237	12 28 51.0	–12 37 12	295.4	+49.7	15.69	0.69	–0.03	0.02	292	4.27	... , ...	1.90	0.99	F
12314–2150	12 31 26.6	–21 50 44	297.6	+40.6	15.41	0.60	0.14	0.04	–10	6.61	... , ...	2.95	4.77	G0
12328–1655	12 32 48.1	–16 55 17	297.5	+45.5	11.75	–0.05	–0.27	0.01	–73	0.27	0.42 , ...	7.84	...	HBB
12375–3244	12 37 31.1	–32 44 47	300.2	+29.8	15.93	–0.08	–0.58	0.10	96	...	0.52 , ...	7.03	0.27	HBB
12380–1558	12 38 01.4	–15 58 36	299.2	+46.5	13.51	–0.09	–0.43	0.02	53 , 0.34	7.62	0.69	HBB
12381–2501	12 38 11.6	–25 01 40	299.9	+37.5	10.95	–0.04	–0.35	0.10	–36	0.29	... , 0.42	8.11	...	HBB
12404–2713	12 40 24.3	–27 13 39	300.7	+35.3	10.31	0.19	–0.31	0.07	16	1.81	... , 0.51	7.49	0.97	?? F+?
12412–1451 ^b	12 41 13.8	–14 51 51	300.2	+47.7	14.80	0.25	0.09	0.02	160	1.78	... , ...	10.51	0.92	HBA
12416–2109 ^c	12 41 36.6	–21 09 10	300.7	+41.4	12.99	0.60	–0.06	0.03	–65	6.14	1.30 , 1.82	3.78	3.93	F7 + late G
12418–1559	12 41 51.1	–15 59 49	300.5	+46.6	14.64	0.40	0.06	0.02	–13	4.34	... , ...	6.90	1.72	A9
12472–1249	12 47 16.9	–12 49 38	302.4	+49.8	16.05	–0.15	–0.42	0.02	265 , ...	7.00	...	HBB
12485–1301	12 48 31.6	–13 01 18	302.8	+49.6	16.00	0.52	–0.23	0.01	312	3.89	... , 0.48	0.50	0.99	F8
12519–2740	12 51 55.6	–27 40 34	303.8	+34.9	14.17	0.64	0.00	0.08	90	8.82	... , ...	1.79	5.36	G1
13020–1709 ^c	13 02 00.0	–17 09 36	307.4	+45.3	15.85	0.72	0.15	0.03	4	8.55	... , 0.38	1.39	4.97	G

TABLE 1. (continued)

Star (1)	RA (1950) (2)	DEC (3)	l (4)	b (5)	V (6)	$B - V$ (7)	$U - B$ (8)	E_{B-V} (9)	VEL (10)	KP (11)	HeI (12)	HP2 (13)	GP (14)	EC Class (15)
13021–3236	13 02 07.4	−32 36 50	306.2	+29.9	11.74	−0.04	−0.23	0.06	33	0.31	... , ...	7.18	0.29	HBB
13040–3229	13 04 01.8	−32 29 25	306.7	+30.0	12.81	−0.09	−0.44	0.05	−29 , ...	5.68	0.39	HBB
13065–2113	13 06 32.4	−21 13 03	308.4	+41.2	16.00	−0.07	−0.27	0.06	164	0.52	0.43 , ...	8.01	0.57	HBB
13090–1631	13 09 04.4	−16 31 12	309.9	+45.8	15.46	0.72	0.34	0.02	1	10.12	... , ...	1.13	6.27	G
13091–3004	13 09 06.4	−30 04 07	308.2	+32.3	15.27	−0.12	−0.40	0.06	65	...	0.52 , 1.06	7.67	...	HBB
13106–2929	13 10 36.6	−29 29 27	308.6	+32.9	13.58	−0.08	−0.42	0.07	−22	0.28	... , ...	7.28	0.59	HBB
13118–2936	13 11 52.2	−29 36 45	308.9	+32.7	16.46	−0.12	−0.35	0.07	195	...	0.67 , 0.34	8.19	0.71	HBB
13121–1524	13 12 11.5	−15 24 49	311.2	+46.8	12.35	−0.05	−0.46	0.02	−7	0.39	... , 0.49	2.46	...	HBB
13150–2723	13 15 02.4	−27 23 40	310.0	+34.8	15.01	−0.02	−0.30	0.04	257	...	0.87 , 0.64	8.67	1.15	HBB
13178–2711 ^e	13 17 53.1	−27 11 53	310.8	+35.0	16.10	0.30	−0.52	0.06	33	3.12	... , 1.12	3.58	3.19	F5
13184–2832	13 18 24.4	−28 32 19	310.8	+33.6	15.69	−0.07	−0.38	0.06	77	0.32	... , 0.70	7.53	0.45	HBB
13205–3209	13 20 33.9	−32 09 52	310.7	+30.0	12.57	0.25	−0.34	0.04	−8	3.43	0.81 , ...	5.78	1.39	F0
13221–1723 ^e	13 22 07.4	−17 23 55	314.1	+44.5	16.45	0.05	−0.58	0.05	135	...	0.49 , 0.95	6.50	...	HBB
13232–2651	13 23 12.6	−26 51 00	312.3	+35.1	15.78	−0.09	−0.42	0.06	211	...	0.76 , 0.56	7.24	...	HBB
13254–2618 ^e	13 25 26.9	−26 18 42	313.1	+35.6	15.11	0.30	−0.42	0.05	6	2.94	... , ...	3.89	1.55	F2
13257–2725	13 25 44.5	−27 25 38	312.9	+34.5	15.88	−0.15	−0.49	0.04	140	0.38	0.29 , 0.38	5.64	0.59	HBB
13271–2015	13 27 06.2	−20 15 25	315.0	+41.5	15.95	−0.04	−0.46	0.06	−48	0.52	0.63 , ...	7.55	...	HBB
13276–1249	13 27 36.4	−12 49 07	317.3	+48.7	12.56	0.57	0.05	0.03	−3	8.18	... , ...	2.81	3.72	F7
13276–1709	13 27 41.7	−17 09 51	316.0	+44.5	15.29	0.40	−0.35	0.05	54	4.20	0.31 , 0.97	3.81	1.01	F2
13277–1229	13 27 44.6	−12 29 25	317.5	+49.0	13.71	0.55	−0.13	0.03	52	6.71	... , ...	3.32	2.65	F8
13277–1245	13 27 47.2	−12 45 30	317.4	+48.8	12.38	0.50	0.01	0.03	−32	7.32	... , ...	3.74	2.60	F5
13293–1947	13 29 21.9	−19 47 54	315.8	+41.8	15.08	0.01	−0.40	0.06	148 , ...	7.03	...	HBB
13309–1303	13 30 59.2	−13 03 39	318.5	+48.3	14.55	0.52	−0.20	0.02	22	6.48	0.94 , ...	2.67	1.29	F4
13314–3233	13 31 28.8	−32 33 15	313.3	+29.2	15.05	0.14	0.17	0.03	−41	1.78	... , 0.90	10.51	1.04	A3
13315–2856	13 31 32.9	−28 56 29	314.1	+32.7	16.45	−0.10	−0.49	0.03	146 , 0.87	7.04	...	HBB
13384–1535	13 38 25.1	−15 35 31	320.1	+45.4	15.06	0.26	0.16	0.06	−109	3.16	0.99 , ...	4.23	1.01	F?
13393–2244	13 39 21.4	−22 44 02	317.9	+38.4	12.53	0.46	−0.18	0.05	7	3.77	... , ...	3.92	0.53	F0
13395–1705	13 39 35.6	−17 05 21	319.9	+43.9	14.64	0.40	−0.31	0.08	−38	3.92	... , 0.35	4.07	1.76	F2
13429–2240	13 42 58.1	−22 40 10	318.9	+38.3	15.22	0.52	0.01	0.06	−107	7.67	... , ...	2.84	3.16	F6
13454–2313	13 45 25.3	−23 13 21	319.4	+37.6	15.91	0.52	−0.37	0.06	31	8.02	... , ...	2.32	5.28	G
13472–2850 ^b	13 47 15.9	−28 50 01	318.1	+32.1	6.18	−0.03	−0.05	0.06	1 , ...	11.45	0.36	A0
13475–1332	13 47 34.5	−13 32 47	324.0	+46.7	15.29	0.63	0.05	0.05	−59	9.32	... , ...	3.79	3.39	G
13494–2253	13 49 27.7	−22 53 08	320.7	+37.6	13.40	0.72	0.25	0.05	−72	7.67	... , ...	1.01	4.66	G4
13494–2327	13 49 28.0	−23 27 04	320.5	+37.1	15.63	0.53	−0.20	0.05	166	1.79	... , ...	3.58	...	F0
13503–1802	13 50 19.3	−18 02 06	322.8	+42.2	14.99	−0.01	−0.08	0.06	−16	0.94	... , ...	8.86	...	HBB/B
13503–2343	13 50 21.8	−23 43 34	320.6	+36.8	15.28	0.01	−0.41	0.05	25 , ...	6.90	...	HBB
13504–2346	13 50 25.0	−23 46 18	320.6	+36.7	13.77	0.71	0.16	0.05	−14	9.14	... , ...	1.44	5.38	G1
13540–2652	13 54 01.4	−26 52 06	320.4	+33.5	14.12	0.70	0.41	0.06	45	9.23	... , 0.41	1.34	5.12	G0
13575–1230	13 57 32.0	−12 30 54	327.8	+46.8	15.67	0.59	−0.07	0.06	−60	8.37	1.25 , 0.28	3.47	3.29	F6
14043–2311	14 04 20.9	−23 11 41	324.6	+36.2	15.87	−0.08	−0.37	0.05	55 , ...	7.81	0.36	HBB

TABLE 1. (continued)

Star (1)	RA (1950) (2)	DEC (3)	l (4)	b (5)	V (6)	$B - V$ (7)	$U - B$ (8)	E_{B-V} (9)	VEL (10)	KP (11)	HeI (12)	HP2 (13)	GP (14)	EC Class (15)
14051–2215	14 05 11.9	–22 15 39	325.2	+37.0	13.11	–0.01	–0.15	0.05	–2, 0.69	8.74	0.60	HBB/B
14078–1745	14 07 48.6	–17 45 21	328.2	+41.0	9.30	0.07	–0.24	0.07	28, 0.52	2.88	...	HBB/B
14118–2728	14 11 49.2	–27 28 31	324.6	+31.6	15.52	0.53	–0.20	0.05	–53	3.43	..., 0.76	3.16	1.30	F4
14146–2144	14 14 38.5	–21 44 16	328.0	+36.7	13.20	0.10	–0.33	0.09	0	1.01	0.50, 0.45	7.10	0.81	HBB
14153–1937	14 15 20.4	–19 37 12	329.3	+38.5	15.83	0.00	–0.53	0.08	–90	0.36	..., ...	9.34	...	HBB
14159–1947	14 15 54.7	–19 47 08	329.4	+38.3	13.09	–0.02	–0.44	0.09	127	...	0.56, 0.55	6.99	...	HBB
14171–1842	14 17 11.8	–18 42 43	330.3	+39.2	15.99	–0.03	–0.43	0.08	141, ...	9.10	...	HBB
14184–2510	14 18 27.0	–25 10 39	327.3	+33.2	15.09	–0.17	–0.32	0.08	–104	0.35	..., 0.69	7.73	...	HBB
14193–2342	14 19 23.3	–23 42 42	328.2	+34.4	16.71	–0.26	–0.62	0.07	68, 1.82	7.01	0.35	HBB
14197–2610	14 19 45.1	–26 10 45	327.1	+32.1	15.16	–0.16	–0.56	0.07	–97	0.52	..., ...	6.48	0.31	HBB
14232–2151	14 23 15.7	–21 51 11	330.2	+35.7	15.65	–0.08	–0.42	0.09	27	0.32	..., 1.02	6.80	0.62	HBB
14255–2015	14 25 33.9	–20 15 08	331.7	+36.9	16.13	–0.08	–0.44	0.08	11	...	0.41, ...	7.15	...	HBB
14258–1257	14 25 53.7	–12 57 06	336.3	+43.3	16.07	0.03	–0.16	0.08	162, ...	8.23	0.41	HBB
14293–1733	14 29 20.7	–17 33 02	334.3	+38.9	15.30	0.01	–0.25	0.08	86	0.49	..., ...	8.08	0.31	HBA
14312–1715	14 31 16.6	–17 15 11	335.0	+38.9	14.14	–0.06	–0.40	0.08	87	0.36	0.50, ...	7.43	...	HBB
14318–0946	14 31 52.9	–09 46 06	340.4	+45.2	16.08	–0.04	–0.37	0.07	193, ...	6.87	0.99	HBB
14324–2020	14 32 28.2	–20 20 02	333.4	+36.1	15.76	0.46	–0.20	0.07	–66	1.41	0.91, ...	4.77	0.52	A–F
14326–1003	14 32 39.6	–10 03 34	340.4	+44.9	14.61	0.47	0.05	0.09	11	3.09	0.57, ...	3.86	1.46	early F
14334–2136	14 33 28.8	–21 36 44	332.9	+34.9	14.48	–0.04	–0.34	0.09	–86, 0.53	7.41	...	HBB
14413–1837	14 41 20.2	–18 37 34	336.7	+36.5	15.65	–0.05	–0.31	0.08	–67	0.70	0.70, 0.25	8.18	...	HBB
14444–1710	14 44 27.5	–17 10 43	338.5	+37.4	14.29	0.54	0.09	0.09	112	6.92	..., ...	3.68	1.23	F2
14464–0734	14 46 27.0	–07 34 01	346.4	+44.9	14.61	0.50	–0.04	0.05	61	6.80	..., ...	4.61	1.51	F2
14491–1028	14 49 09.9	–10 28 27	344.7	+42.2	15.95	–0.06	–0.41	0.07	–28, 0.98	7.00	...	HBB
14495–1632	14 49 35.6	–16 32 44	340.2	+37.2	15.73	0.04	–0.42	0.10	–18	0.78	..., ...	7.14	1.05	HBB
14496–2048 ^e	14 49 39.4	–20 48 33	337.3	+33.6	13.46	0.33	–0.43	0.11	19	3.29	..., ...	5.58	1.46	F2
14497–1619	14 49 47.6	–16 19 54	340.4	+37.4	15.16	0.98	0.47	0.10	3	10.35	0.45, 1.61	0.82	7.08	G–K
14520–1648	14 52 00.9	–16 48 55	340.6	+36.7	14.71	0.66	0.13	0.10	–9	7.99	..., ...	1.81	4.10	F8
14521–0821	14 52 06.2	–08 21 41	347.2	+43.5	15.99	–0.04	–0.39	0.07	–91, 0.50	7.63	0.92	HBB
14537–0832	14 53 46.7	–08 32 20	347.5	+43.1	13.27	–0.02	–0.30	0.06	36	0.67	0.28, 0.32	6.71	...	HBB
14566–1736 ^e	14 56 40.8	–17 36 25	341.2	+35.4	16.40	0.40	–0.35	0.10	127	3.79	0.25, ...	5.04	...	F
14579–1759	14 57 54.7	–17 59 12	341.2	+34.9	16.07	0.56	–0.14	0.10	81	4.52	0.59, 0.28	5.04	2.25	F2
15001–1646	15 00 08.1	–16 46 57	342.6	+35.6	14.74	–0.03	–0.35	0.10	33	...	0.29, ...	7.73	...	HBB/B9
15012–0943	15 01 17.9	–09 43 17	348.4	+41.0	15.42	0.70	0.27	0.08	–9	7.74	1.26, 0.56	3.25	3.85	G
15255–1716	15 25 30.2	–17 16 12	347.9	+31.4	15.66	0.57	–0.07	0.11	–10	5.53	1.06, ...	1.86	3.35	G
15278–1732 ^b	15 27 53.3	–17 32 39	348.2	+30.8	15.77	0.56	0.01	0.09	–4	6.92	..., ...	1.46	3.00	G
15284–1737	15 28 25.5	–17 37 23	348.3	+30.7	13.98	0.58	–0.04	0.09	–21	7.56	..., ...	1.97	2.39	G
15292–1716	15 29 14.2	–17 16 00	348.7	+30.8	15.15	0.62	–0.01	0.09	–14	6.89	0.76, 0.69	2.16	3.86	G
15354–1250	15 35 24.8	–12 50 29	353.5	+33.0	15.14	–0.01	–0.25	0.13	–7, ...	7.64	0.43	HBB
15354–1513	15 35 29.3	–15 13 27	351.6	+31.3	16.65	–0.16	–0.52	0.09	104	0.59	..., 0.59	5.18	0.88	B5/HBB
15374–1552	15 37 27.9	–15 52 50	351.5	+30.5	14.89	0.02	–0.24	0.09	–83	0.53	0.42, 0.32	7.94	0.71	HBB

TABLE 1. (continued)

Star (1)	RA (1950) (2)	DEC (3)	l (4)	b (5)	V (6)	$B - V$ (7)	$U - B$ (8)	E_{B-V} (9)	VEL (10)	KP (11)	HeI (12)	HP2 (13)	GP (14)	EC Class (15)
15400–1323 ^b	15 40 03.2	–13 23 32	354.0	+31.8	15.16	0.45	0.19	0.13	33	1.67	... , ...	7.32	1.19	A/HBB
15472–1341	15 47 17.1	–13 41 38	355.2	+30.4	13.15	0.03	–0.15	0.14	81	0.34	0.36 , ...	9.46	0.29	HBA
19137–6211	19 13 43.4	–62 11 15	334.3	–26.8	15.72	–0.07	–0.49	0.04	63	0.27	0.91 , ...	8.13	0.76	HBB
19199–6638 ^b	19 19 55.4	–66 38 36	329.4	–28.0	13.48	0.63	0.09	0.06	15	9.06	... , ...	2.42	3.56	F6
19207–7045	19 20 45.5	–70 45 56	324.8	–28.4	15.16	–0.05	–0.46	0.07	–72	0.36	1.32 , 0.57	6.55	...	HBB
19239–6640	19 23 54.2	–66 40 41	329.4	–28.4	11.98	0.55	–0.03	0.06	26	7.59	... , ...	3.67	2.60	F7
19250–6014	19 25 01.8	–60 14 58	336.7	–27.9	15.66	–0.08	–0.43	0.05	231	0.42	0.25 , 0.41	8.51	0.66	HBB
19274–6127	19 27 24.8	–61 27 05	335.4	–28.4	16.42	–0.05	–0.51	0.06	72 , ...	6.64	...	HBB
19329–7548	19 32 57.4	–75 48 03	319.0	–29.2	15.90	–0.08	–0.62	0.07	62 , 0.88	6.44	...	HBB
19332–7151 ^b	19 33 12.5	–71 51 52	323.5	–29.4	14.72	0.49	0.10	0.06	372	1.36	... , ...	4.47	0.39	~F5
19337–6743	19 33 43.4	–67 43 59	328.3	–29.4	9.43	0.01	–0.13	0.08	–30 , 0.25	10.02	0.28	B9/A0
19343–6315	19 34 21.4	–63 15 16	333.4	–29.3	16.04	–0.12	–0.60	0.06	32	...	0.59 , 1.04	6.40	...	HBB
19345–7132	19 34 30.6	–71 32 03	323.9	–29.5	13.72	–0.06	–0.33	0.06	47 , ...	7.41	...	HBB/A0
19384–5737	19 38 26.3	–57 37 22	339.9	–29.4	13.36	0.55	–0.08	0.03	–9	7.74	... , 0.38	3.19	2.76	F6
19388–5429	19 38 52.0	–54 29 32	343.5	–29.1	16.30	–0.15	–0.67	0.04	12	...	0.50 , 0.87	5.53	...	lateB/HBB
19413–3806	19 41 19.2	–38 06 14	1.7	–26.2	15.72	–0.16	–0.78	0.11	–51	...	0.43 , 0.41	3.88	...	B3/HBB
19418–5714	19 41 48.2	–57 14 42	340.4	–29.8	14.40	0.43	–0.16	0.04	–189	3.09	... , ...	4.26	1.04	F0
19425–5735	19 42 34.1	–57 35 14	340.0	–29.9	14.75	0.61	–0.09	0.04	–2	8.90	... , ...	3.72	4.16	F7
19434–5538	19 43 25.6	–55 38 32	342.2	–29.9	15.51	–0.13	–0.55	0.04	–27	0.57	1.11 , ...	6.80	0.92	HBB
19467–7700	19 46 43.3	–77 00 37	317.5	–29.9	15.58	0.02	–0.52	0.09	239	0.29	0.66 , 0.91	6.38	...	HBB
19485–6208	19 48 31.7	–62 08 34	334.8	–30.9	16.47	–0.14	–0.49	0.03	64	...	0.60 , ...	6.93	...	HBB
19490–7708	19 49 04.6	–77 08 32	317.4	–30.0	12.86	–0.02	–0.48	0.09	1 , ...	6.65	...	HBB/B8?
19504–5752	19 50 28.5	–57 52 30	339.7	–31.0	14.82	–0.09	–0.51	0.02	101	...	0.36 , ...	7.10	0.80	HBB
19541–5049	19 54 10.1	–50 49 00	348.0	–30.9	14.79	0.16	0.14	0.04	108	4.76	... , 0.25	6.38	1.46	F0
19543–4231	19 54 19.1	–42 31 34	357.5	–29.7	12.72	–0.01	–0.23	0.06	57	0.50	0.57 , ...	9.31	...	A0
19552–4334	19 55 13.4	–43 34 44	356.3	–30.0	14.32	–0.10	–0.51	0.04	99	0.43	... , ...	7.03	0.34	HBB
19584–4727	19 58 29.5	–47 27 13	352.0	–31.2	10.80	–0.11	–0.50	0.04	17	0.36	0.31 , ...	6.99	0.43	HBB/A0?
19585–4229	19 58 34.4	–42 29 04	357.7	–30.4	13.02	0.26	0.11	0.06	–53	4.49	... , ...	7.06	1.41	~F1
19596–5356	19 59 37.1	–53 56 35	344.4	–32.0	14.37	–0.12	–0.59	0.05	–185	0.27	0.71 , 1.14	6.61	0.84	B5/HBB
20002–5324	20 00 12.4	–53 24 37	345.1	–32.1	15.69	–0.12	–0.63	0.05	–96	0.27	0.90 , 0.98	6.73	0.62	HBB
20013–5436	20 01 22.6	–54 36 46	343.7	–32.3	15.55	–0.11	–0.64	0.05	–39	9.31	... , ...	1.09	5.19	G
20028–4411	20 02 52.1	–44 11 39	355.9	–31.5	14.55	–0.02	–0.42	0.02	74	0.81	0.45 , ...	7.57	...	A0
20036–6224	20 03 36.8	–62 24 29	334.4	–32.6	13.95	0.46	–0.18	0.02	134	2.60	0.56 , ...	4.21	...	~A8
20060–2725	20 06 03.3	–27 25 16	14.9	–28.2	15.19	0.00	–0.49	0.12	150	0.48	0.27 , 0.70	5.42	...	HBB
20064–4547	20 06 27.0	–45 47 55	354.1	–32.4	15.11	–0.16	–0.59	0.00	74	0.36	... , ...	4.91	...	HBB?
20064–7128	20 06 29.3	–71 28 24	323.7	–32.0	14.51	0.68	0.25	0.05	–50	8.96	... , ...	1.15	5.21	G0
20074–7241	20 07 27.3	–72 41 08	322.3	–31.9	11.80	0.50	0.00	0.04	–29	7.43	0.34 , ...	3.88	2.70	~F5
20077–6205	20 07 47.5	–62 05 37	334.8	–33.1	14.51	0.58	0.16	0.02	23	9.00	0.29 , ...	1.65	3.95	~F8
20084–4850	20 08 24.3	–48 50 40	350.6	–33.0	15.11	0.82	0.16	0.03	–42	10.22	... , 0.35	3.46	6.05	G
20089–6511	20 08 56.8	–65 11 08	331.1	–33.0	11.34	–0.21	–0.83	0.04	70 , ...	7.43	...	HBB/HBA

TABLE 1. (continued)

Star (1)	RA (1950) (2)	DEC (3)	l (4)	b (5)	V (6)	$B - V$ (7)	$U - B$ (8)	E_{B-V} (9)	VEL (10)	KP (11)	HeI (12)	HP2 (13)	GP (14)	EC Class (15)
20101–2837	20 10 07.9	–28 37 22	13.9	–29.4	15.10	–0.09	–0.25	0.12	67, 0.25	7.83	...	HBB/A0
20114–2927	20 11 24.8	–29 27 54	13.1	–29.9	16.07	–0.04	–0.61	0.09	–33	...	0.57, 0.69	6.83	0.92	HBB
20131–4714	20 13 08.5	–47 14 43	352.6	–33.7	15.07	–0.08	–0.54	0.02	121	0.71	0.52, ...	6.54	...	HBB
20132–7317 ^a	20 13 14.6	–73 17 55	321.5	–32.2	12.19	0.31	–0.43	0.05	21	4.24	..., 0.39	4.55	1.58	~F2
20134–6159	20 13 24.8	–61 59 15	334.8	–33.8	15.32	–0.05	–0.47	0.03	183	...	0.62, 0.83	7.04	...	HBB
20139–4308	20 13 56.7	–43 08 30	357.5	–33.3	14.77	–0.10	–0.54	0.03	–37, 1.23	7.00	...	HBB
20161–3223	20 16 10.4	–32 23 38	10.1	–31.7	14.93	0.01	–0.56	0.10	–186	0.34	..., ...	6.89	...	HBB
20178–7215	20 17 48.3	–72 15 41	322.6	–32.7	12.62	0.46	–0.07	0.04	21	6.99	..., 0.36	3.78	1.61	~F2
20179–4633	20 17 54.3	–46 33 19	353.5	–34.4	15.17	–0.15	–0.57	0.00	11, ...	5.92	...	HBB
20230–7240	20 23 04.0	–72 40 11	322.0	–33.0	11.82	0.60	0.02	0.03	64	7.24	..., 0.29	2.81	3.15	~F8
20237–2528	20 23 46.4	–25 28 12	18.4	–31.3	14.81	–0.07	–1.01	0.06	163, ...	5.73	...	HBB?
20239–6246	20 23 57.2	–62 46 08	333.7	–34.9	11.93	0.59	–0.04	0.03	–15	7.98	..., ...	3.08	3.43	F7
20264–4934	20 26 26.3	–49 34 44	349.9	–36.0	11.81	–0.11	–0.43	0.02	91, ...	7.29	...	HBB
20275–1409	20 27 31.8	–14 09 30	31.0	–28.1	14.89	–0.04	–0.24	0.05	–22	0.39	..., 0.69	8.09	0.45	HBB
20278–1727	20 27 48.3	–17 27 26	27.5	–29.5	14.88	0.54	–0.12	0.04	–214	4.28	..., ...	1.95	1.74	mid F
20279–1520 ^e	20 27 54.2	–15 20 34	29.8	–28.7	13.30	0.55	0.00	0.07	–56	...	0.38, 0.48	8.09	0.42	HBB
20281–1519	20 28 09.5	–15 19 54	29.8	–28.7	14.47	0.43	–0.17	0.07	–273	4.23	..., ...	3.44	0.91	early F
20283–5535	20 28 21.4	–55 35 46	342.4	–36.2	14.53	–0.08	–0.57	0.05	100	0.56	0.69, 0.32	6.64	...	HBB
20286–1638	20 28 36.4	–16 38 25	28.5	–29.3	15.22	0.04	–0.15	0.06	–61	0.36	..., ...	9.48	...	HBA
20289–4248	20 28 59.7	–42 48 45	358.3	–36.0	15.79	–0.10	–0.57	0.02	–205	...	0.57, 0.52	6.78	0.81	HBB
20290–3057	20 29 05.5	–30 57 18	12.6	–34.0	16.38	–0.10	–0.53	0.05	–42	0.48	0.55, ...	7.56	...	HBB
20303–2741	20 30 21.0	–27 41 54	16.4	–33.4	14.86	0.50	–0.01	0.04	1	8.19	..., ...	2.69	2.79	~F7
20305–6923 ^b	20 30 32.1	–69 23 47	325.7	–34.4	14.44	0.17	0.15	0.04	95	3.78	0.28, ...	3.92	0.99	F1
20312–1742	20 31 16.6	–17 42 24	27.6	–30.3	14.66	0.51	–0.10	0.03	7	6.45	..., ...	2.77	1.82	early F
20314–4106	20 31 27.7	–41 06 59	0.4	–36.3	15.32	0.81	0.39	0.02	90	9.98	..., 1.22	0.73	5.87	G?
20328–5219 ^d	20 32 48.2	–52 19 28	346.5	–37.0	15.23	–0.05	–0.25	0.00	62	0.64	..., 0.31	6.93	1.44	B7/HBB
20331–3141	20 33 10.6	–31 41 15	11.9	–35.0	12.78	0.30	0.11	0.05	26	2.74	..., ...	9.42	0.95	~A3
20362–1732	20 36 16.9	–17 32 35	28.3	–31.4	15.16	0.52	–0.28	0.04	–121	2.58	..., 0.73	3.33	3.68	~F7
20373–1637	20 37 19.5	–16 37 20	29.4	–31.3	14.48	0.56	–0.09	0.05	–50	6.12	..., ...	1.71	2.09	mid F
20385–1715	20 38 33.1	–17 15 44	28.9	–31.8	14.45	0.53	–0.06	0.05	–229	6.09	..., ...	3.11	2.17	mid F
20393–1727	20 39 19.3	–17 27 41	28.7	–32.0	14.86	–0.01	–0.45	0.04	–52, 0.36	7.55	0.53	HBB
20421–1633	20 42 06.4	–16 33 26	30.0	–32.3	15.60	0.37	–0.09	0.04	–268	1.93	0.38, ...	7.62	0.90	HBA
20422–1556 ^e	20 42 17.1	–15 56 30	30.7	–32.1	12.31	0.32	–0.47	0.04	14	1.72	..., 0.34	3.78	2.03	early F
20432–1454	20 43 16.5	–14 54 41	31.9	–31.9	13.16	0.70	0.18	0.05	–53	9.79	..., ...	1.99	4.63	F–G
20443–2814	20 44 19.2	–28 14 44	16.8	–36.5	15.25	0.15	0.21	0.09	–178	1.99	..., ...	7.74	1.37	~A3
20448–2727	20 44 50.3	–27 27 52	17.7	–36.4	14.96	0.53	0.14	0.11	–261	2.62	..., ...	6.01	0.36	A4
20449–1730	20 44 55.3	–17 30 10	29.3	–33.3	15.50	–0.13	–0.11	0.05	–220	0.35	..., ...	8.95	0.43	HBA?
20464–1630 ^e	20 46 28.9	–16 30 36	30.5	–33.2	15.02	0.29	–0.58	0.04	–57	1.60	..., ...	5.29	1.55	mid F
20477–1659	20 47 47.1	–16 59 35	30.1	–33.7	14.62	0.45	0.06	0.06	–43	3.99	..., 0.29	7.50	1.30	early F
20484–1744	20 48 29.2	–17 44 48	29.4	–34.2	14.05	0.60	0.05	0.04	–6	8.61	..., ...	1.96	4.35	late F–G

TABLE 1. (continued)

Star (1)	RA (1950) (2)	DEC (3)	l (4)	b (5)	V (6)	$B - V$ (7)	$U - B$ (8)	E_{B-V} (9)	VEL (10)	KP (11)	HeI (12)	HP2 (13)	GP (14)	EC Class (15)
20515-6735	20 51 31.2	-67 35 21	327.2	-36.7	14.62	0.04	-0.01	0.02	8	0.56	... , ...	9.30	0.32	HBA
20546-6817	20 54 40.1	-68 17 35	326.2	-36.8	14.34	0.56	-0.15	0.02	56	7.03	... , ...	2.83	3.08	~F7
20568-3239 ^e	20 56 49.5	-32 39 38	12.0	-40.1	13.84	0.48	-0.16	0.08	-80	1.69	... , ...	4.37	0.62	late A?
20573-2922	20 57 22.9	-29 22 36	16.2	-39.6	16.09	0.83	0.05	0.11	6	8.32	... , 0.36	3.36	4.23	~F8
21003-3119	21 00 22.1	-31 19 14	13.9	-40.6	15.54	0.63	0.07	0.09	79	9.35	... , 0.29	0.87	5.45	G
21004-5753	21 00 28.2	-57 53 10	338.8	-40.2	15.57	-0.07	-0.57	0.05	1	0.49	0.25 , 0.38	6.12	...	HBB
21040-7421 ^b	21 04 01.1	-74 21 05	318.9	-35.2	13.86	0.21	0.12	0.06	55	2.77	... , ...	4.87	1.32	late A
21070-5811	21 07 03.7	-58 11 54	338.1	-41.0	14.72	-0.11	-0.35	0.03	118	0.42	0.43 , 0.59	7.17	0.48	HBB
21108-2616	21 10 48.8	-26 16 07	21.1	-41.7	14.48	-0.07	-0.52	0.06	22	...	0.67 , 0.84	6.24	0.28	~B5/HBB
21306-7230	21 30 40.1	-72 30 58	319.8	-37.7	14.60	-0.09	-0.34	0.02	196	0.29	... , 0.50	8.09	...	HBB
21589-2743	21 58 55.4	-27 43 55	22.3	-52.5	12.70	0.46	-0.14	0.00	-11	5.80	... , ...	2.95	2.42	~F5
21591-7353 ^e	21 59 08.1	-73 53 15	316.9	-38.6	14.46	0.07	-0.81	0.03	36	8.92	... , 0.31	2.00	5.50	F-G
22011-7350	22 01 10.9	-73 50 22	316.8	-38.7	14.02	0.60	0.02	0.03	48	7.78	... , ...	2.44	2.23	F-G
22150-6551	22 15 05.7	-65 51 11	324.0	-44.8	13.28	-0.14	-0.51	0.00	-84 , 0.31	6.83	...	HBB
22168-2246	22 16 48.7	-22 46 51	32.0	-55.4	13.89	-0.26	-0.94	0.01	17	0.28	... , ...	6.12	...	HBB
22270-8220	22 27 03.2	-82 20 46	308.3	-33.5	14.41	0.69	0.05	0.10	28	9.69	... , ...	2.00	4.83	FG
22351-8200	22 35 07.7	-82 00 04	308.3	-34.0	12.09	0.60	0.12	0.11	87	5.63	... , 0.70	3.11	0.92	~F0
22438-8416	22 43 50.8	-84 16 02	306.5	-32.3	12.48	0.69	0.20	0.07	41	8.44	... , ...	2.98	3.98	~F8
22536-2724	22 53 36.5	-27 24 25	26.2	-64.4	14.78	-0.07	-0.53	0.02	-37	0.25	... , ...	6.90	...	HBB
22572-5059	22 57 16.8	-50 59 44	337.2	-58.4	14.42	0.60	-0.06	0.00	9	8.86	0.42 , 0.46	1.57	3.98	G
23011-2744	23 01 10.1	-27 44 51	25.9	-66.1	15.56	0.45	-0.20	0.00	-5	1.89	... , 0.74	2.56	0.38	F?
23048-1600	23 04 48.1	-16 00 09	52.9	-63.3	15.09	0.76	0.20	0.02	1	8.09	1.65 , 0.56	...	5.84	G
23053-1432	23 05 19.0	-14 32 40	55.8	-62.7	15.22	0.56	-0.17	0.02	38	7.07	... , ...	1.36	3.65	~F6
23053-4838 ^b	23 05 19.6	-48 38 24	339.3	-60.8	13.94	0.35	-0.87	0.00	81	4.83	... , ...	3.35	2.17	~A5
23062-1559	23 06 13.1	-15 59 29	53.3	-63.6	14.92	0.56	-0.01	0.02	13	8.11	... , ...	2.97	4.69	G
23065-1600	23 06 35.8	-16 00 49	53.3	-63.7	16.14	0.52	-0.17	0.02	-107	5.70	0.53 , ...	4.14	1.86	~F4
23076-1544	23 07 41.2	-15 44 15	54.2	-63.8	16.08	0.47	-0.15	0.02	-39	4.13	... , ...	1.96	1.01	~F5
23077-1610	23 07 47.4	-16 10 27	53.4	-64.0	15.32	0.58	-0.03	0.02	-146	8.30	... , 1.23	1.89	3.63	~F8
23093-2728	23 09 19.4	-27 28 06	27.0	-67.9	15.16	0.47	-0.17	0.04	-10	6.12	... , 0.31	5.46	2.16	~F5
23113-5055 ^b	23 11 22.0	-50 55 33	334.5	-60.1	13.51	0.33	0.03	0.00	110	1.86	... , ...	6.05	0.63	~A4
23143-2919	23 14 18.9	-29 19 29	22.1	-69.1	15.24	0.44	-0.31	0.00	-18	1.92	... , ...	2.17	0.88	~F2
23231-2352	23 23 09.0	-23 52 21	38.5	-70.4	15.71	-0.22	-0.52	0.01	-8	...	0.36 , ...	6.72	1.02	HBB
23330-2431	23 33 02.4	-24 31 26	38.3	-72.7	15.32	-0.10	-0.85	0.01	-26	...	0.64 , 0.97	2.70	0.45	~B4/HBB?
23348-2254	23 34 52.3	-22 54 10	43.9	-72.7	14.71	-0.07	-0.38	0.01	-137 , 0.31	7.70	0.50	HBB
23473-2340 ^a	23 47 22.4	-23 40 35	44.6	-75.6	14.37	0.29	-0.50	0.01	-54	2.00	... , 0.50	3.84	2.58	F5

^aBinary ?

^bVariable ?

^cEclipsing Binary ?

^dPeculiar ?

^eComposite ?

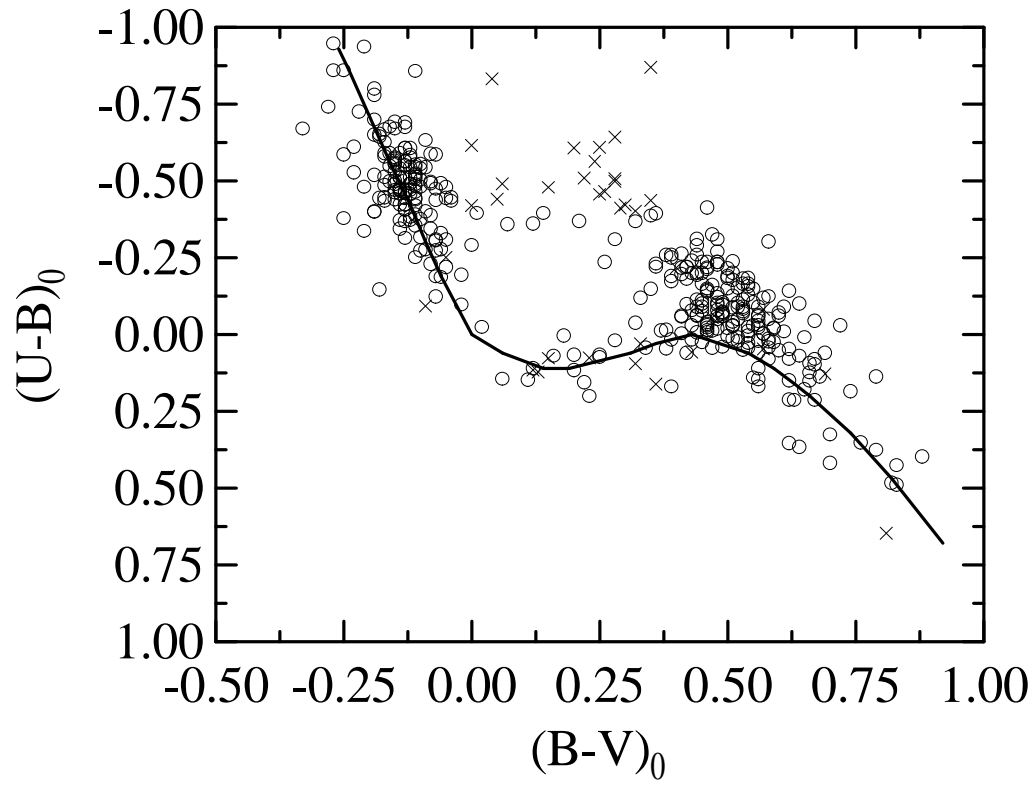


TABLE 2. Previous identifications for EC program stars

Star	HD	BD/CD/CPD	BPS	Other
00237–2317	Ton S 157
00381–1423	CS 31062–0022	PB 8463
01510–3919	SB 774
03240–6229	...	CPD–62 272
03289–0304	HD 21867	BD–03 565
03436–4748	LB 1689
03462–5813	HD 24101	CD–58 758
04224–5424	LP 1723
04300–5341	LB 1735
04460–3215	HIP 120411
05438–4741	LB 1789
05515–6231	HD 40021	CD–62 221
10275–1547	BS 17582–0061	...
10299–1555	BS 17582–0081	...
11100–1813	HD 97411	BD–17 3321	...	HIP 54742
12270–3205	V* BP Hya
12381–2501	...	CD–24 10477
12404–2713	HD 110528	CD–26 9290
12416–2109	SV 5914
13472–2850	SV 6460
14078–1745	HD 123884
14334–2136	CS 22871–0046	...
14413–1837	CS 22871–0086	...
14496–2048	CS 22871–0102	...
14537–0832	PG 1453–085
15354–1513	LB 870
15400–1323	SV 7206
19137–6211	CS 22891–0177	...
19332–7151	V* EV Pav
19337–6743	HD 184308	CD–67 2351	...	HIP 96624
19434–5538	CS 22896–0175	...
19504–5752	CS 22873–0035	...
19584–4727	HD 189424	CD–47 13211
20064–4547	CS 22943–0090	...
20089–6511	HD 191351
20139–4308	CS 22943–0054	...
20179–4633	CS 22943–0086	...
20237–2528	CS 22955–0070	...
20275–1409	CS 22950–0140	...
20286–1638	CS 22950–0157	...
20305–6923	V* IZ Pav
20331–3141	CS 30336–0092	...
20432–1454	HD 197743	BD–15 5783
21040–7421	SV 13581
21108–2616	CS 30331–0072	...
22150–6551	CS 22956–0103	...
22536–2724	Ton S 79
23053–4838	V* AO Gru
23113–5055	V* AP Gru
23231–2352	CS 30315–0060	Ton S 98, PHL 515
23330–2431	Ton S 104, PHL 564
23348–2254	Ton S 105, PHL 567
23473–2340	CS 29499–0052	...

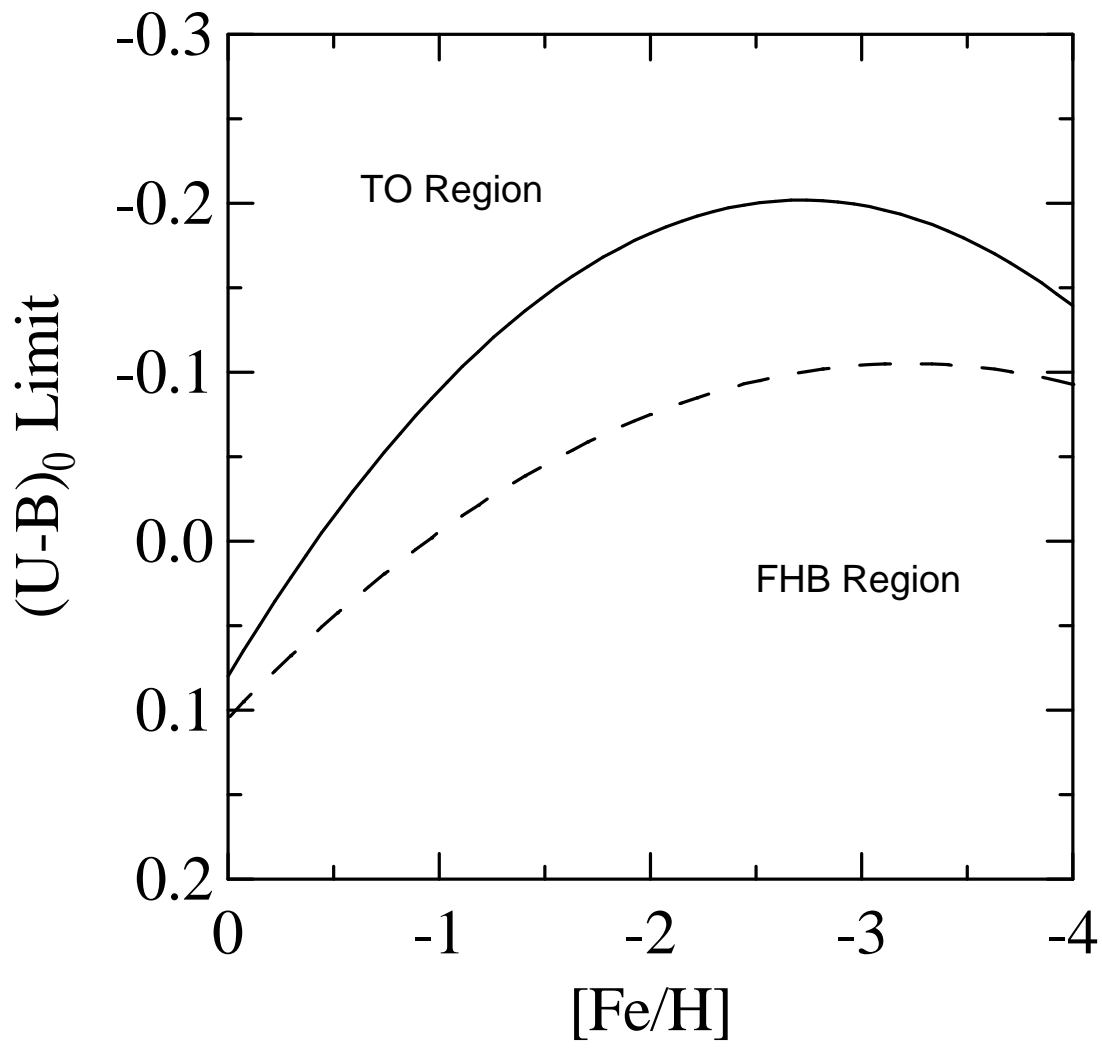


TABLE 3. Line index wavelength bands (\AA)

Line	Line Band	Blue Sideband	Red Sideband
Ca II- <i>K</i> 6	3930.7–3936.7	3903.0–3923.0	4000.0–4020.0
Ca II- <i>K</i> 12	3927.7–3939.7	3903.0–3923.0	4000.0–4020.0
Ca II- <i>K</i> 18	3924.7–3942.7	3903.0–3923.0	4000.0–4020.0
He I-4026	4020.2–4032.2	4000.0–4020.0	4144.0–4164.0
H δ - <i>HD</i> 12	4095.8–4107.8	4000.0–4020.0	4144.0–4164.0
H δ - <i>HD</i> 24	4089.8–4113.8	4000.0–4020.0	4144.0–4164.0
G-band	4297.5–4312.5	4247.0–4267.0	4362.0–4372.0
He I-4471	4465.7–4477.7	4415.0–4435.0	4490.0–4510.0

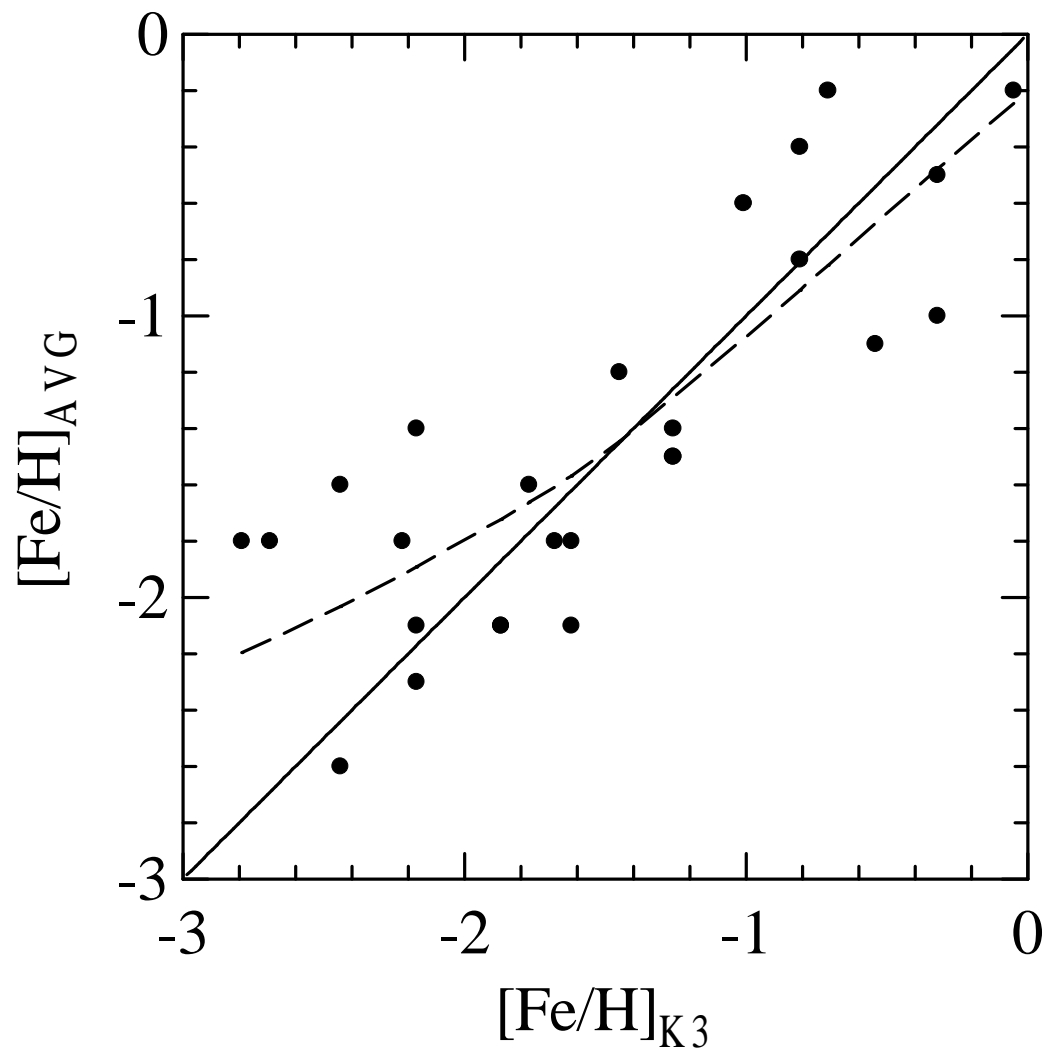


TABLE 4. Probable HBB stars

Star	Star	Star
00237–2317	13221–1723:	20060–2725
00269–5602	13257–2725	20064–4547
00538–8121	13315–2856	20089–6511
01510–3919	14153–1937	20114–2927
02518–6611	14193–2342	20131–4714
03436–4748	14197–2610	20139–4308
03495–7850	14496–2048:	20161–3223
04224–5424	15354–1513	20179–4633
04300–5341	19137–6211	20237–2528
05077–6225	19207–7045	20283–5535
05107–7724	19274–6127	20289–4248
05138–5914	19329–7548	20290–3057
05190–3512	19343–6315	20464–1630:
05515–6231	19388–5429	21004–5753
05581–5856	19413–3806	21108–2616
06012–7810	19434–5538	21591–7353:
09076–1141	19467–7700	22150–6551
09433–1526	19485–6208	22168–2246
10153–1731	19490–7708	22536–2724
11344–2713	19504–5752	23053–4838:
11475–2259	19552–4334	23231–2352
12040–3226	19584–4727	23330–2431
12258–1353	19596–5356	23473–2340:
12375–3244	20002–5324	
13178–2711:	20013–5436	

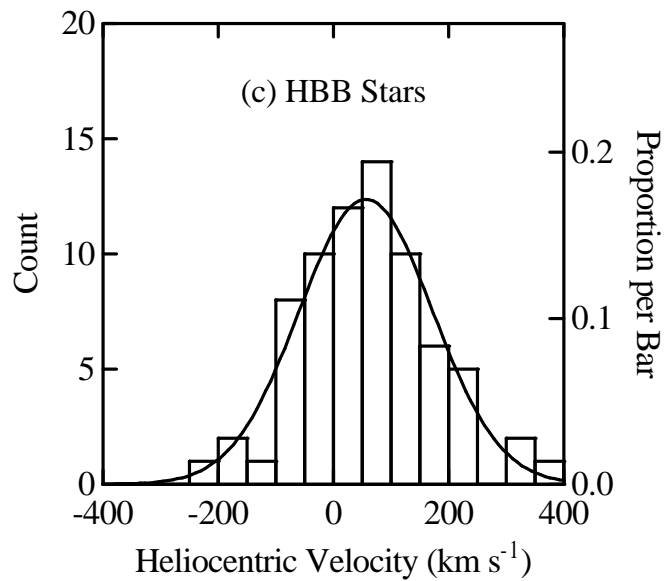
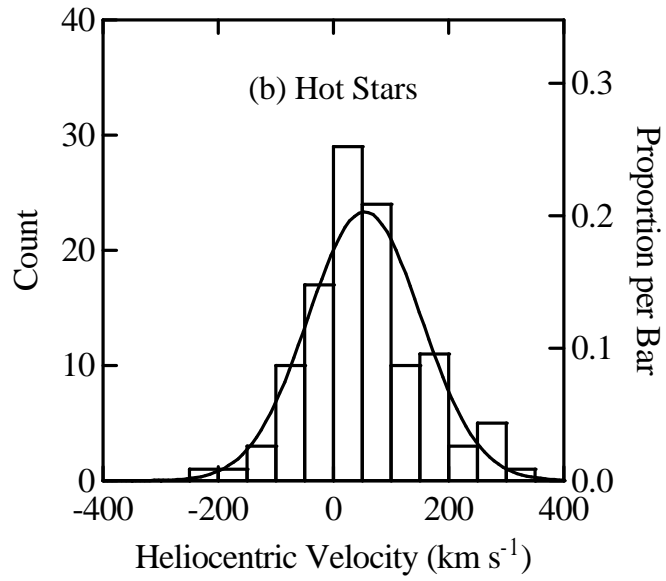
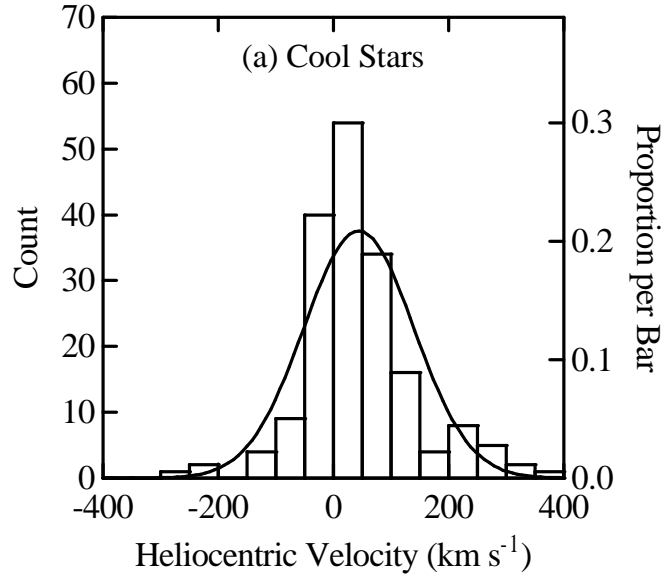


TABLE 5. Physical parameter estimates – EC hot stars

Star (1)	T_{eff} (K) (2)	$\log g$ (3)	$[\text{Fe}/\text{H}]_{\text{WK}}$ (4)	$[\text{Fe}/\text{H}]_{\text{CTA}}$ (5)	$[\text{Fe}/\text{H}]_{\text{MTA}}$ (6)	$[\text{Fe}/\text{H}]_{\text{AVG}}$ (7)	$\Delta[\text{Fe}/\text{H}]$ (8)	Class (9)	M_V (10)	Dist (11)	Notes (12)
00097–3243	6700	4.7	−1.7	−1.5	−1.3	−1.6	0.2	A	3.74	3400	
00179–6503	9100:	3.8:	0.0	−2.4	−1.1	−0.6:	1.1	A:	1.36	4000	
00381–1423	9700	2.8	−3.0	−3.0	−0.7	−3.0	0.0	FHB	1.24	4400	
03240–6229	9600	3.1	−2.5	−2.8	−0.7	−2.7	0.3	FHB	1.56	800	
03289–0304	6900	4.2	−0.2	−0.2	0.0	−0.2	0.0	A	3.35	100	
03462–5813	9600:	3.1:	−2.2	−2.8	−1.3	−2.5:	0.6	FHB	1.77	400	
03572–3729	7600	4.1	0.0	−0.1	−0.1	−0.1	0.0	A	2.54	1200	
04420–1908	9600:	2.4:	−0.7	−1.0	−1.7	−0.9:	0.4	FHB	1.73	1900	
04460–3215	8000:	2.5:	−1.5	−1.7	−1.2	−1.6:	0.2	FHB:	0.92	1400	
05084–2919	9800	3.3	0.0	0.0	...	FHB/A	
05131–6050	9600:	2.4:	−3.0	−0.2	−1.9	−2.4:	1.1	FHB	1.60	7500	
05198–4005	9800:	3.1:	0.0	0.0	−1.2	0.0:	0.0	FHB	2.25	5000	
05438–4741	9800:	2.9:	−0.4	−0.4:	...	FHB	2.39	1100	
05581–6201	9400:	2.9:	−0.8	−0.6	−1.6	−0.7:	0.2	FHB	2.46	4900	
05587–5808	7400	4.8	−2.4	−2.5	−1.3	−2.4	0.0	A	3.38	2200	r
06031–7744	7300:	2.3:	−0.1	−1.7	−1.8	−1.7:	0.1	FHB:	0.69	5600	
06250–7842	6500	4.3	−3.0	−2.2	−1.6	−2.6	0.8	A	3.92	1700	r
06353–7725	7100	4.7	−0.1	−0.2	−0.6	−0.2	0.1	A	2.75	1300	
09088–1116	9500:	2.9:	−3.0	−1.2	−2.1	−1.6:	0.9	FHB	1.84	4500	
09120–1155	9800	2.9	−1.0	−0.6	−1.6	−0.8	0.4	FHB	2.97	3600	
09290–1650	6600:	3.5:	−3.0	−3.0	−3.0	−3.0:	0.0	A:	3.84	3400	r
09479–0931	7400:	4.7:	−1.9	−0.8	−0.6	−0.7:	0.2	A:	2.78	2400	r
10008–0749	7600	4.9	−0.3	−0.7	0.0	−0.1	0.3	A	2.54	3500	
10165–1232	9500:	2.9:	0.0	−0.6	−0.7	−0.7:	0.1	FHB	2.34	1800	
10185–0947	6500	4.5	−2.5	−2.1	−3.0	−2.3	0.4	A	4.15	2300	r
10197–1231	7200	2.3	−1.8	−1.5	−1.3	−1.4	0.2	FHB	0.76	4800	
10221–1929	9700:	2.9:	0.0	−0.7	−0.7	−0.7:	0.0	FHB	2.45	900	
10275–1547	9900	2.8	−0.1	−0.1	...	FHB	2.04	1100	
10291–2653	9900:	2.6:	−0.4	−0.4	...	FHB	2.18	1900	
10292–0957	6300	2.2	−1.8	−1.3	−0.9	−1.1	0.4	FHB	0.76	3900	r
10298–2231	6900	4.8	−1.6	−1.2	−3.0	−1.4	0.4	A	3.51	3100	r
10299–1555	9000	2.9	−0.4	−1.6	−1.3	−1.4	0.3	FHB	1.89	1300	
10548–1451	7800	4.6	−1.3	−1.7	0.0	−1.5	0.4	Am	2.30	1900	
10568–2257	7100	2.8	−1.0	−1.6	−1.7	−1.6	0.1	FHB	0.66	8400	
10588–1632	6900:	4.9:	−1.1	−0.9	−0.2:	−1.0	0.2	Am:	2.75	1500	
11006–2213	7400	3.3	−1.2	−1.1	−3.0	−1.1	0.1	A	2.56	5900	
11013–2547	6600	2.2	−1.9	−1.8	−2.1	−1.8	0.1	FHB	0.62	7600	
11024–3246	9700	2.8	−0.1	−0.1	−0.8	−0.1	0.1	FHB	1.66	7300	
11034–1758	9900	2.9	0.0	0.0	...	FHB	1.89	1300	
11100–1813	9800	3.8	0.0	0.0	...	FHB/A	
11183–2731	6400	3.6	−2.0	−1.6	−2.3	−2.1	0.4	A	4.11	2300	
11196–3155	8200	3.3	−0.8	−1.0	−0.8	−0.8	0.0	FHB/A	
11221–2844	7100	2.4	−3.0	−2.7	−2.4	−2.9	0.3	FHB	0.46	5600	
11222–2606	9000	2.6	−1.5	−1.5	−2.9	−1.5	0.0	FHB	1.97	4500	
11337–3043	9700:	2.9:	0.0	−0.6	−2.5	−0.3:	0.6	FHB	2.53	1300	
11348–2735	7000:	4.7:	−0.6	−0.6	−0.8	−0.6:	0.0	A:	3.16	2800	
11366–3217	8900	2.9	−0.5	−2.0	−1.5	−1.8	0.6	FHB	3.11	3600	r
11372–2938	9600:	2.9:	0.0	−1.5	−0.7	−0.4:	0.7	FHB	2.78	900	
11417–2110	9500:	2.9:	0.0	−1.0	−2.8	−0.5:	1.0	FHB	2.37	1200	r
11471–3219	6900	4.5	−1.5	−1.6	−2.1	−1.6	0.1	A	3.92	500	

TABLE 5. (continued)

Star (1)	T_{eff} (K) (2)	$\log g$ (3)	$[\text{Fe}/\text{H}]_{\text{WK}}$ (4)	$[\text{Fe}/\text{H}]_{\text{CTA}}$ (5)	$[\text{Fe}/\text{H}]_{\text{MTA}}$ (6)	$[\text{Fe}/\text{H}]_{\text{AVG}}$ (7)	$\Delta[\text{Fe}/\text{H}]$ (8)	Class (9)	M_V (10)	Dist (11)	Notes (12)
12000–1549	7100	2.4	−1.9	−1.9	−1.6	−1.9	0.0	FHB	0.60	8500	
12225–1928	9600:	2.9:	0.0	0.0	0.0	0.0:	0.0	FHB	2.15	5800	
12256–2707	8000:	2.7:	−1.1	−0.8	−0.9	−0.9:	0.2	FHB:	1.03	13000	r
12266–1557	7100	3.9	−0.5	−0.5	−1.9	−0.5	0.0	A	2.86	2100	
12270–3205	7700:	2.8:	−1.9	−1.7	−1.2	−1.8:	0.3	FHB:	0.73	8200	R
12328–1655	9400	2.8	0.0	−1.3	−1.4	−1.4	0.2	FHB	1.48	1100	
12380–1558	9500:	2.9:	−1.3	−1.7	0.0	−1.5:	0.4	Am	0.17	5400	
12381–2501	9800:	3.1:	0.0	0.0:	...	FHB	2.47	500	
12404–2713	7700	2.5	−1.2	−1.5	−0.7	−1.3	0.3	FHB	0.85	800	
12412–1451	7900:	3.9:	−0.8	−1.1	−0.9	−0.8:	0.1	A:	2.58	2800	
12418–1559	6800	2.6	−1.0	−1.2	−1.2	−1.2	0.0	FHB	0.74	6000	r
12472–1249	9500	2.9	−1.5	−1.6	−1.7	−1.5	0.0	FHB	2.55	5000	
13021–3236	9900	2.7	0.0	0.0	...	FHB	2.06	900	
13040–3229	9500:	2.4:	0.0	−1.1	−0.7	−0.9:	0.3	FHB	2.30	1300	
13065–2113	6400	4.8	−3.0	−3.0	−2.8	−3.0	0.0	A	0.45	13000	r
13091–3004	9200:	2.9:	−1.4	−1.5	−1.7	−1.5:	0.1	FHB	2.70	3300	
13106–2929	8900:	2.6:	−1.3	−1.6	−1.8	−1.4:	0.3	FHB	2.32	1800	
13118–2936	9100	2.9	0.0	−2.5	−3.0	−2.7	0.5	FHB	2.61	5900	
13121–1524	9600:	2.6:	−0.3	−1.5	−1.9	−1.7:	0.4	FHB	1.49	1500	
13150–2723	9700	3.0	0.0	−3.0	−3.0	−3.0	0.0	FHB	1.17	5900	
13184–2832	9600	3.1	−3.0	−1.1	−1.5	−1.3	0.4	FHB	2.11	5200	
13205–3209	7700	4.2	−0.4	−0.6	−0.0	−0.5	0.2	A	2.40	1100	
13232–2651	9500:	2.9:	0.0	−1.5	−1.2	−1.3:	0.3	FHB	2.34	4900	
13254–2618	7800:	4.6:	0.0	−0.5	−2.5	−0.3:	0.5	A:	2.46	3400	
13271–2015	9700:	3.1:	0.0	0.0	−1.6	0.0:	0.0	FHB	2.05	6000	
13276–1709	6900	4.8	−1.3	−0.8	−1.6	−1.5	0.3	A	3.48	2300	r
13293–1947	9700:	2.5:	−0.1	−0.2	−0.1	−0.1:	0.0	FHB	1.66	4800	
13314–3233	8000	3.1	−1.0	−1.1	−1.5	−1.0	0.1	FHB	0.89	6800	
13384–1535	7100	2.2	−1.7	−1.5	−3.0	−1.6	0.2	FHB	0.67	7600	
13395–1705	7100	4.9	−1.0	−0.7	−0.8	−0.8	0.0	A	2.95	2200	
13472–2850	9800:	3.9:	−1.4	−1.4:	...	A:	0.68	100	
13503–1802	9700:	3.1:	0.0	0.0	−1.6	0.0:	0.0	FHB	1.81	4300	
13503–2343	9400:	2.9:	−0.1	−0.8	−1.3	−1.0:	0.6	FHB	1.41	5900	
14043–2311	9600	3.1	−0.7	−1.4	−3.0	−1.1	0.7	FHB	2.15	5500	
14051–2215	9800	3.1	−0.3	−0.3	...	FHB	1.69	1900	
14078–1745	6600	4.7	−3.0	−3.0	−3.0	−3.0	0.0	A	2.13	300	r
14146–2144	8300	2.2	−0.5	−1.4	−1.5	−1.5	0.1	FHB	1.09	2600	r
14159–1947	9600:	3.1:	−0.4	−1.1	−0.6	−0.5:	0.2	FHB	2.05	1600	
14171–1842	9600:	3.4:	−0.1	−2.7	0.0	−0.1:	0.1	FHB/A	
14184–2510	8900:	2.6:	−1.3	−1.4	−1.7	−1.3:	0.2	FHB	3.93	1700	r
14232–2151	9100:	2.6:	−3.0	−1.5	−3.0	−3.0:	0.0	FHB	2.28	4700	
14255–2015	9600:	2.9:	0.0	−1.1	−1.9	−1.5:	0.8	FHB	2.43	5500	
14258–1257	9900	3.1	0.0	0.0	...	FHB	1.67	7600	
14293–1733	9700	3.3	0.0	−0.3	−2.8	−0.1	0.3	FHB/A	
14312–1715	9700:	2.9:	0.0	−0.4	−2.5	−0.2:	0.4	FHB	2.43	2200	
14318–0946	9300	2.4	−3.0	−3.0	−1.0	−3.0	0.0	FHB	1.58	7900	
14324–2020	6900	4.7	−1.7	−1.9	−2.2	−1.8	0.2	A	3.93	2300	
14326–1003	6400	2.2	−2.1	−1.9	−2.2	−2.1	0.1	FHB	0.56	6500	
14334–2136	9000	2.6	−0.9	−1.8	−1.6	−1.7	0.2	FHB	2.04	3100	
14413–1837	9700	3.4	0.0	0.0	−3.0	0.0	0.0	FHB/A	

TABLE 5. (continued)

Star (1)	T_{eff} (K) (2)	$\log g$ (3)	$[\text{Fe}/\text{H}]_{\text{WK}}$ (4)	$[\text{Fe}/\text{H}]_{\text{CTA}}$ (5)	$[\text{Fe}/\text{H}]_{\text{MTA}}$ (6)	$[\text{Fe}/\text{H}]_{\text{AVG}}$ (7)	$\Delta[\text{Fe}/\text{H}]$ (8)	Class (9)	M_V (10)	Dist (11)	Notes (12)
14491–1028	9500:	2.6:	−3.0	−2.3	−2.2	−2.3:	0.2	FHB	1.93	6400	
14495–1632	9400:	2.8:	0.0	−0.1	−2.7	0.0:	0.1	FHB	1.73	6300	
14521–0821	9600:	3.1:	−0.6	−1.9	−1.3	−1.6:	0.5	FHB	1.85	6700	
14537–0832	9700	2.7	0.0	0.0	−1.4	0.0	0.0	FHB	1.89	1900	
14566–1736	7400:	4.7:	−0.3	−0.5	−1.7	−0.4:	0.2	A:	2.36	5400	
15001–1646	9600:	3.1:	−0.9	−1.6	−2.1	−1.8:	0.5	FHB	2.01	3500	
15354–1250	9700:	2.9:	−2.0	−1.4	−0.2	−1.7:	0.6	Am	0.63	14000	
15374–1552	9700	3.0	0.0	−0.2	−0.8	−0.1	0.2	FHB	1.79	4200	
15400–1323	7200:	2.3:	−1.6	−1.9	−1.3	−1.8:	0.3	FHB:	0.69	7800	
15472–1341	6400	4.2	−3.0	−3.0	−3.0	−3.0	0.0	A	0.79	3000	r
19250–6014	9700:	3.4:	0.0	−0.5	−0.7	−0.6:	0.2	FHB/A	
19337–6743	9900	3.5	−3.0	−3.0	...	FHB/A	
19345–7132	9600	2.9	−0.3	−1.3	−0.7	−0.5	0.4	FHB	2.16	2000	
19418–5714	6300	3.6	−2.2	−2.0	−3.0	−2.1	0.2	A	4.08	1200	r
19541–5049	7100	2.3	−0.9	−0.7	−1.1	−0.8	0.2	FHB	0.91	6000	
19543–4231	9700	3.3	0.0	−0.7	−1.4	−0.4	0.7	FHB/A	
19585–4229	7400	3.5	−0.2	−0.5	−0.2	−0.2	0.1	A	2.26	1400	
20028–4411	9100	2.5	0.0	−1.1	−1.1	−1.1	0.0	FHB	1.41	4300	
20101–2837	8500	2.3	−0.2	−2.2	−3.0	−2.6	0.9	FHB	2.96	2700	r
20132–7317	7700:	4.7:	−0.3	−0.1	0.0	−0.1:	0.1	A:	2.43	900	
20134–6159	9700:	2.6:	−1.7	−1.6	−1.2	−1.7:	0.1	FHB	1.57	5600	
20264–4934	9600:	2.9:	0.0	−1.7	−2.4	−2.0:	0.7	FHB	1.97	900	
20275–1409	9800	3.0	0.0	0.0	...	FHB	1.97	3800	
20281–1519	6600	4.8	−1.6	−1.5	−1.5	−1.5	0.1	A	3.56	1500	
20286–1638	8900	3.1	−1.6	−1.8	−2.0	−1.7	0.1	FHB	1.14	6500	
20305–6923	7300:	2.3:	−1.3	−1.0	−1.2	−1.3:	0.1	FHB:	0.81	5300	r,R
20328–5219	9900:	2.6:	0.0	0.0:	...	FHB:	1.67	5100	
20331–3141	7600	3.6	−1.1	−1.1	−0.7	−1.1	0.0	A	2.78	1000	
20393–1727	9700:	2.8:	−3.0	−1.6	−3.0	−3.0:	0.0	FHB	1.10	5600	
20421–1633	7400	4.2	−1.3	−1.6	−0.7	−1.4	0.3	A	3.34	2800	
20422–1556	7500:	4.7:	−1.2	−1.5	−0.4:	−1.4	0.3	Am:	2.62	900	r
20443–2814	7500	2.1	−1.5	−1.5	−1.6	−1.5	0.1	FHB	0.91	7400	r
20449–1730	6900	4.6	−2.9	−3.0	−3.0	−3.0	0.0	A	0.56	16000	r
20477–1659	6300	2.5	−1.8	−1.7	−1.1	−1.8	0.2	FHB	0.63	6300	r
20515–6735	9000	3.5	−1.3	−1.4	−1.0	−1.4	0.1	FHB/A	
20568–3239	6900:	4.5:	−1.8	−2.1	−1.8	−1.8:	0.0	A:	4.09	900	
21040–7421	7600:	3.2:	−0.9	−1.2	−1.0	−1.0:	0.1	FHB:	0.84	4000	r
21070–5811	9900	2.9	0.0	0.0	...	FHB	2.47	2800	
21306–7230	9600	3.1	0.0	−0.9	−1.7	−1.3	0.8	FHB	1.91	3500	
23113–5055	6700:	2.4:	−2.1	−2.1	−2.2	−2.1:	0.0	FHB:	0.56	3900	R
23348–2254	9700	3.1	−0.5	−0.9	−0.9	−0.9	0.1	FHB	1.72	4000	

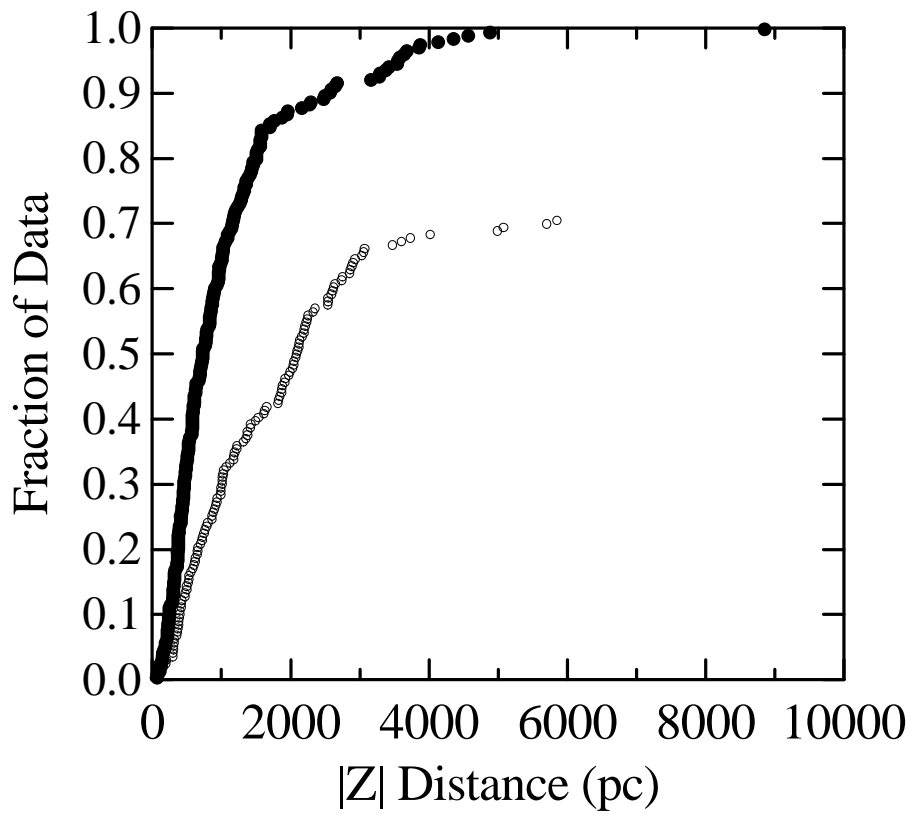


TABLE 6. Derived quantities – EC cool stars

Star	Class	M_V	Distance	$[\text{Fe}/\text{H}]_{\text{K3}}$
00097–3243	SG	3.27	4192	–2.44 (0.18)
00230–2340	TO	4.64	766	–0.44 (0.27)
00316–2543	TO	4.23	1332	–0.55 (0.15)
00341–7725	TO	4.46	593	–0.98 (0.15)
00347–7711	TO	4.52	927	–1.11 (0.15)
00448–6351	SG	3.60	1211	–1.35 (0.29)
00594–6309	TO/FHB	4.58 (0.75)	340 (1982)	–1.11: (0.15)
01021–6222	SG	3.65	1565	–0.88 (0.34)
01030–5232	FHB	0.58	9784	–2.04 (0.15)
01181–7826	TO	4.47	636	–1.26 (0.15)
01218–5735	G	2.40	1991	–1.77 (0.27)
01218–5741	SG	3.55	576	–1.51 (0.29)
01226–6746	TO	4.76	697	–1.00 (0.16)
01233–2807	G	2.46	2855	–0.71 (0.37)
01327–6630	TO	4.80	908	–1.71 (0.15)
01497–6658	TO	4.22	687	–1.07 (0.15)
02023–7847	TO	4.62	745	–2.54 (0.17)
02133–5827	G	–0.30	16129	–1.87 (0.37)
02317–2144	TO	4.52	1272	–0.68 (0.17)
02368–1725	TO	4.78	1300	–2.19 (0.15)
02536–3218	SG	3.93	1385	–0.48 (0.33)
03148–4056	TO	4.82	1825	–2.94 (0.26)
03224–3558	SG	3.46	710	–1.98 (0.15)
03289–0304	SG	4.06	92	–0.71 (0.15)
03330–7735	SG	3.50	1734	–1.64 (0.26)
03528–3734	TO	4.59	691	–1.97 (0.15)
03546–3737	TO	4.75	404	–0.67 (0.21)
03547–3738	TO	4.69	613	–1.00 (0.16)
03569–3728	TO	4.61	247	–0.84 (0.16)
03597–3727	TO	3.58	661	–0.46 (0.15)
03598–3742	TO	4.58	437	–0.44 (0.20)
03599–3723	TO	4.84	549	–0.30 (0.29)
04005–3742	TO	4.27	547	–0.69 (0.15)
04009–3721	TO/FHB	4.71 (0.75)	416 (2600)	–1.15: (0.15)
04013–3746	TO	4.79	208	–0.64 (0.28)
04026–3726	SG	3.88	510	–0.70 (0.31)
04040–8518	G	2.96	2266	–1.18 (0.37)
04359–2745	TO	4.79	921	–0.36 (0.23)
04571–3729	TO	4.34	1009	–0.69 (0.15)
04573–1506	TO/FHB	4.23 (0.72)	1599 (8037)	–1.29: (0.15)
04578–3749	TO	4.55	1225	–1.66 (0.15)
04580–3726	TO	4.79	1005	–0.36 (0.23)
05002–1314	TO	5.02	555	–1.53 (0.15)
05024–7723	TO	4.89	860	–1.02 (0.21)
05028–7725	TO	3.63	803	–0.37 (0.15)
05039–3423	TO	4.60	1033	–0.85 (0.25)
05053–3342	TO	4.53	1140	–1.39 (0.15)
05063–2330	G	–3.53	31734	–2.79 (0.15)
05067–7720	TO	3.51	1944	+0.28 (0.17)
05070–2725	TO/FHB	4.52 (0.75)	587 (3320)	–1.11: (0.15)

TABLE 6. (continued)

Star	Class	M_V	Distance	$[\text{Fe}/\text{H}]_{\text{K3}}$
05094–3103	TO	4.94	382	−1.65 (0.15)
05098–3047	TO	4.64	1093	−0.44 (0.27)
05101–3607	TO	4.74	988	−1.57 (0.15)
05116–3357	TO	4.87	948	−1.28 (0.15)
05117–3559	TO	4.58	925	−1.73 (0.15)
05121–7726	SG	3.40	2376	−1.86 (0.15)
05331–4234	TO/FHB	4.74 (0.71)	1202 (7682)	−1.33: (0.15)
05344–5747	TO	4.89	583	−1.02 (0.21)
05377–5834	SG	3.42	1665	−2.16 (0.15)
06250–7842	SG	3.27	1801	−2.44 (0.18)
06353–7725	SG	4.31	503	−0.05 (0.26)
06360–7721	TO	1.79	3670	+0.27 (0.22)
09222–1243	TO	4.69	219	−1.02 (0.21)
09227–1245	TO	4.84	543	−1.02 (0.21)
09278–1246	TO	4.16	1637	−0.55 (0.15)
09288–1234	SG	3.46	2315	−1.84 (0.22)
09306–1222	TO	4.55	1476	−1.66 (0.15)
09340–1725	G	3.22	1479	−1.48 (0.30)
09423–0936	SG	3.60	1703	−0.88 (0.38)
09490–1611	FHB	0.60	7506	−1.98 (0.15)
09550–1554	TO	4.46	1087	−2.10 (0.15)
09555–1208	SG	3.37	2035	−1.81 (0.15)
09561–1334	TO	4.51	1508	−2.02 (0.15)
10087–1227	TO/FHB	3.76 (0.89)	1165 (4366)	−0.37: (0.15)
10115–2144	TO	4.66	831	−0.44 (0.20)
10163–1238	TO	3.24	970	+0.02 (0.17)
10185–0947	SG	3.34	3160	−2.17 (0.18)
10195–1740	TO	3.94	1249	−0.71 (0.15)
10213–1737	TO	4.51	229	−0.53 (0.17)
10269–2548	TO	5.04	795	−2.19 (0.15)
10289–0951	TO/FHB	4.38 (0.83)	324 (1661)	−0.69: (0.15)
10292–0957	TO	3.08	1270	−0.54 (0.18)
10298–2231	SG	3.81	2442	−1.26 (0.17)
10381–2731	TO/FHB	4.60 (0.48)	1863 (12401)	−2.54: (0.17)
10391–2043	TO	4.76	659	−1.32 (0.18)
10393–2105	TO	3.80	613	−0.59 (0.15)
10405–1648	SG	3.58	2711	−1.35 (0.29)
10419–1959	SG	3.64	471	−1.48 (0.22)
10435–2140	TO	5.22	712	−1.03 (0.28)
10471–2455	SG	3.31	1350	−2.37 (0.15)
10496–2452	TO	5.36	528	−1.20 (0.28)
10548–2724	SG	3.50	430	−1.07 (0.35)
10582–2256	TO	3.90	865	−0.50 (0.15)
10588–1632	SG:	4.23	719	−0.32: (0.23)
11013–2547	FHB	0.65	7014	−1.68 (0.26)
11033–2344	FHB	0.46	9012	−2.61 (0.18)
11057–2051	TO	4.55	829	+0.06 (0.24)
11063–2349	TO/FHB	4.36 (0.61)	1325 (7469)	−1.88: (0.15)
11082–2831	G	2.62	1426	−0.94 (0.39)
11084–2607	FHB	0.69	6640	−1.48 (0.15)

TABLE 6. (continued)

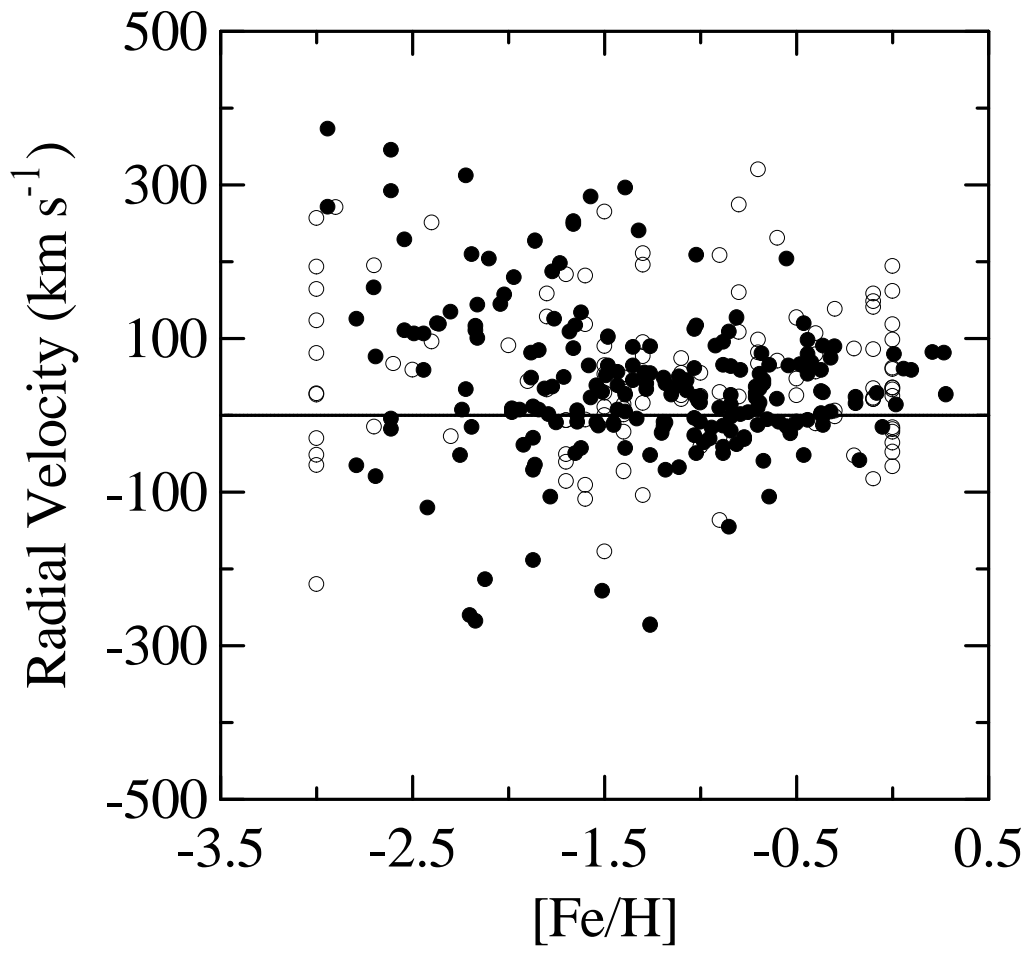
Star	Class	M_V	Distance	$[\text{Fe}/\text{H}]_{\text{K3}}$
11092–2933	TO	4.57	955	−1.28 (0.15)
11107–3237	TO	4.02	432	−0.95 (0.15)
11109–1514	TO	4.56	1275	−2.69 (0.20)
11138–1507	SG	3.38	2221	−2.36 (0.15)
11163–1635	TO	4.54	1521	−1.39 (0.15)
11183–2731	SG	3.63	2610	−1.62 (0.15)
11249–1723	TO	5.20	1206	−0.42 (0.35)
11267–3200	G	2.74	2180	−1.39 (0.33)
11340–1830	G	1.93	6129	−2.49 (0.20)
11348–2735	SG:	3.92	1780	−1.01: (0.15)
11362–2157	G:	−0.14	18792	−1.94: (0.33)
11374–2223	TO/FHB	4.25 (0.79)	494 (2423)	−0.90: (0.15)
11405–1807	SG	3.38	2249	−2.16 (0.15)
11413–1838	TO	3.77	2321	+0.21 (0.21)
11471–3219	SG	3.47	541	−1.77 (0.18)
12021–1744	TO	4.39	2182	−1.76 (0.15)
12037–2710	TO	4.84	1381	−2.24 (0.15)
12226–2211	TO	4.15	2171	+0.10 (0.24)
12238–1855	G	1.84	3305	−0.79 (0.39)
12266–1557	TO	1.99	3041	−0.32 (0.23)
12272–1657	FHB	0.69	2395	−1.54 (0.15)
12288–1237	G	0.95	8615	−2.61 (0.17)
12314–2150	SG	3.43	2353	−1.75 (0.16)
12416–2109	SG:	3.42	787	−1.86: (0.15)
12418–1559	FHB	0.70	5992	−1.45 (0.15)
12485–1301	SG	3.31	3405	−2.22 (0.15)
12519–2740	TO	4.81	666	−0.36 (0.23)
13020–1709	SG:	3.21	3226	−1.39: (0.33)
13090–1631	SG	3.84	2045	−0.79 (0.39)
13276–1249	TO	4.87	333	−0.84 (0.21)
13276–1709	TO	3.73	1909	−1.26 (0.17)
13277–1229	TO	4.76	591	−1.49 (0.15)
13277–1245	TO/FHB	4.24 (0.82)	408 (1967)	−0.77: (0.15)
13309–1303	TO	4.62	941	−1.57 (0.15)
13393–2244	TO	4.43	388	−1.84 (0.15)
13395–1705	SG	3.97	1213	−0.81 (0.18)
13429–2240	TO	4.08	1552	−0.64 (0.15)
13454–2313	TO	3.68	2563	−0.37 (0.15)
13475–1332	TO	4.70	1222	−0.17 (0.25)
13494–2253	G	2.19	1627	−1.87 (0.25)
13494–2327	SG	3.36	2649	−2.70 (0.24)
13504–2346	SG	3.63	996	−0.88 (0.36)
13540–2652	SG	3.80	1064	−0.67 (0.34)
13575–1230	TO	4.68	1450	−0.67 (0.21)
14118–2728	SG	3.31	2581	−2.25 (0.15)
14324–2020	SG	3.17	2979	−2.79 (0.21)
14326–1003	FHB	0.62	5548	−1.87 (0.17)
14444–1710	FHB	0.78	4450	−1.03 (0.15)
14464–0734	TO	4.23	1107	−1.03 (0.15)
14497–1619	G	0.96	5994	−0.75 (0.38)

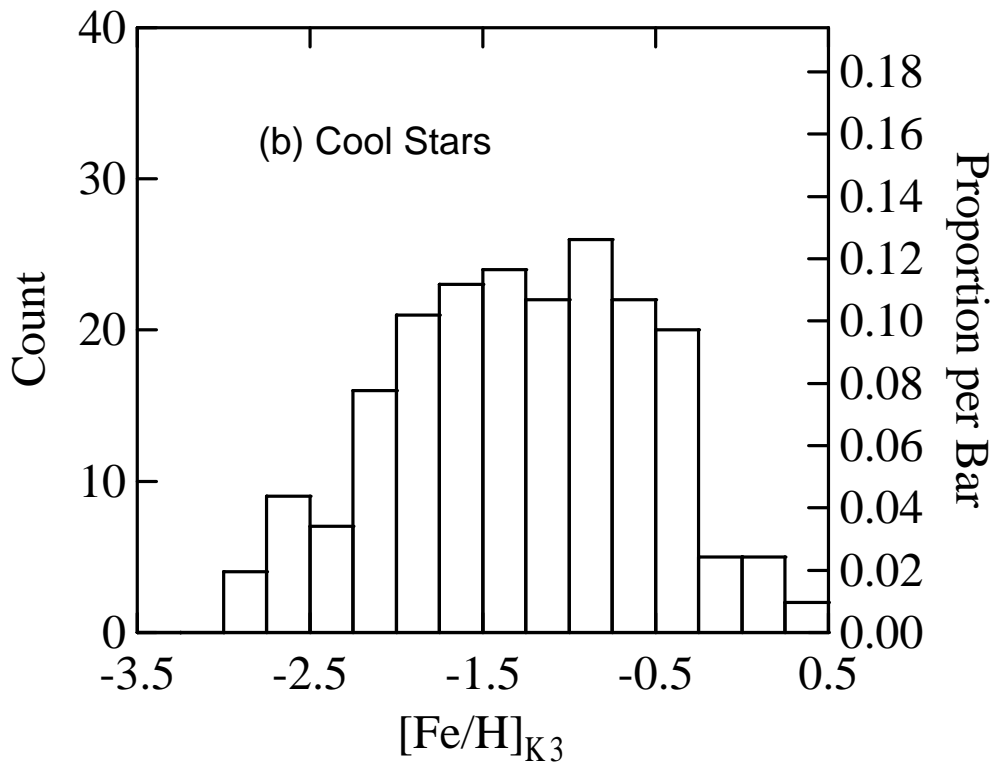
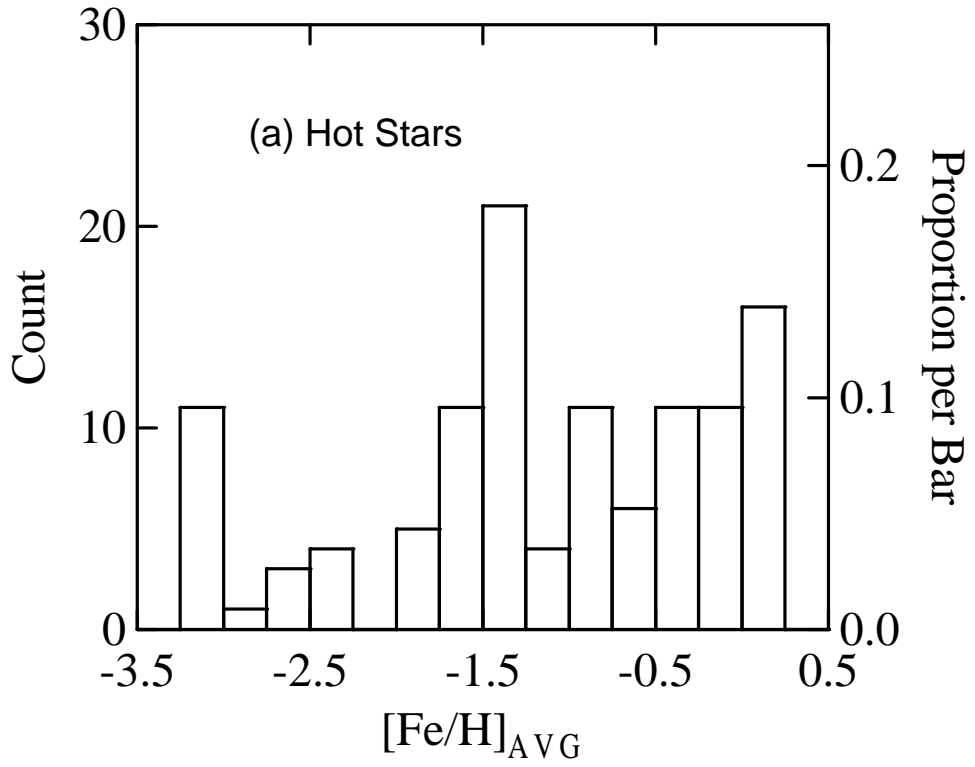
TABLE 6. (continued)

Star	Class	M_V	Distance	$[\text{Fe}/\text{H}]_{\text{K3}}$
14520–1648	TO	5.03	752	−1.19 (0.24)
14566–1736	SG:	3.97	2651	−0.81: (0.18)
14579–1759	TO	4.48	1804	−1.88 (0.15)
15012–0943	SG	3.51	2151	−1.64 (0.26)
15255–1716	TO	4.64	1370	−1.54 (0.15)
15278–1732	TO/FHB:	4.37 (0.77)	1674 (8797)	−1.03: (0.15)
15284–1737	TO	4.46	711	−0.84 (0.15)
15292–1716	TO	4.97	957	−1.53 (0.15)
15400–1323	FHB:	0.54	6965	−2.22: (0.26)
19199–6638	TO:	4.65	535	−0.19: (0.22)
19239–6640	TO	4.42	298	−0.84 (0.15)
19332–7151	FHB:	0.39	6689	−2.94: (0.26)
19384–5737	TO	4.73	506	−1.00 (0.16)
19418–5714	SG	3.45	1465	−1.87 (0.17)
19425–5735	TO	4.87	897	−0.36 (0.23)
20036–6224	TO	4.69	692	−2.30 (0.15)
20064–7128	SG	3.71	1346	−0.88 (0.34)
20074–7241	TO/FHB	4.18 (0.82)	317 (1464)	−0.77: (0.15)
20077–6205	TO	4.58	940	−0.19 (0.22)
20084–4850	G	2.38	3363	−0.88 (0.39)
20178–7215	TO	3.60	604	−0.60 (0.15)
20230–7240	SG	3.61	418	−1.58 (0.20)
20239–6246	TO	4.96	226	−1.19 (0.24)
20278–1727	SG	3.37	1895	−2.12 (0.15)
20281–1519	SG	3.81	1230	−1.26 (0.17)
20303–2741	TO	3.68	1626	−0.37 (0.15)
20312–1742	TO	4.74	926	−1.43 (0.15)
20314–4106	G	2.08	4316	−0.92 (0.39)
20362–1732	SG	3.33	2191	−2.42 (0.17)
20373–1637	TO	4.85	786	−1.65 (0.15)
20385–1715	TO/FHB	4.79 (0.68)	798 (5289)	−1.51: (0.15)
20421–1633	TO	4.05	1930	−2.17 (0.26)
20432–1454	SG	4.04	623	−0.46 (0.35)
20448–2727	FHB	0.55	6523	−2.20 (0.15)
20477–1659	FHB	0.67	5693	−1.62 (0.15)
20484–1744	TO	4.59	740	−0.65 (0.25)
20546–6817	TO	4.96	730	−1.43 (0.17)
20568–3239	SG:	3.21	1195	−2.69: (0.20)
20573–2922	G	1.80	6176	−1.64 (0.31)
21003–3119	TO	3.97	1814	+0.01 (0.18)
21589–2743	TO	4.59	419	−1.45 (0.15)
22011–7350	TO	5.12	578	−1.19 (0.24)
22270–8220	TO	4.56	812	−0.08 (0.25)
22351–8200	FHB	0.66	1659	−1.66 (0.15)
22438–8416	SG	3.63	531	−1.18 (0.30)
22572–5059	TO	5.16	711	−0.70 (0.31)
23011–2744	SG	3.25	2904	−2.61 (0.18)
23048–1600	G	1.12	6055	−1.79 (0.29)
23053–1432	TO	4.96	1097	−1.43 (0.17)
23062–1559	TO	4.84	1008	−0.84 (0.21)

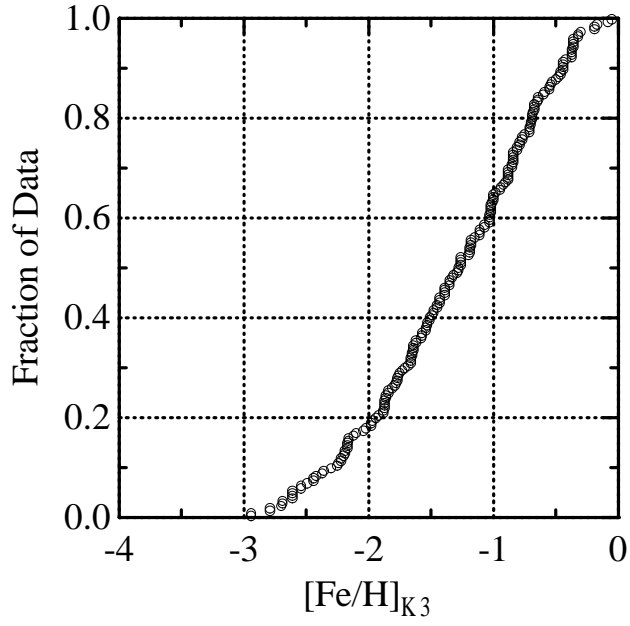
TABLE 6. (continued)

Star	Class	M_V	Distance	$[\text{Fe}/\text{H}]_{\text{K3}}$
23065–1600	TO	4.92	1706	−1.78 (0.15)
23076–1544	TO	4.36	2148	−1.92 (0.15)
23077–1610	TO	4.71	1285	−0.85 (0.25)
23093–2728	TO	4.15	1503	−1.18 (0.15)
23113–5055	FHB:	0.55	3903	−2.17: (0.26)
23143–2919	TO	4.85	1199	−2.61 (0.18)

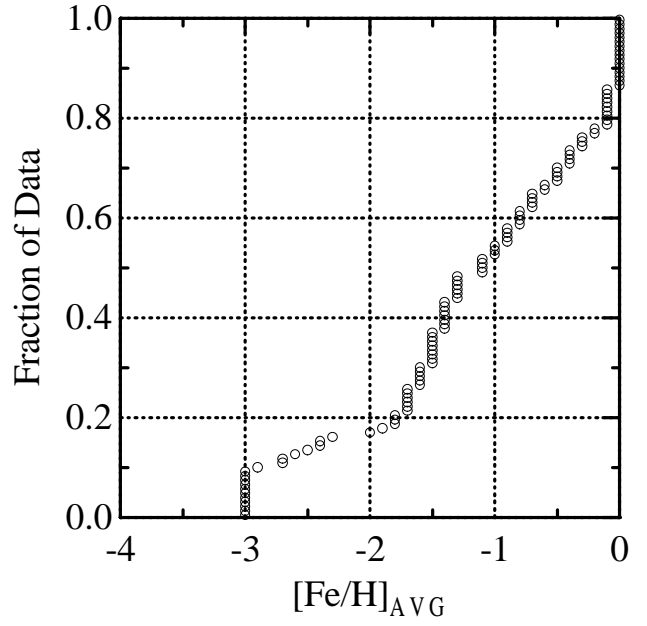




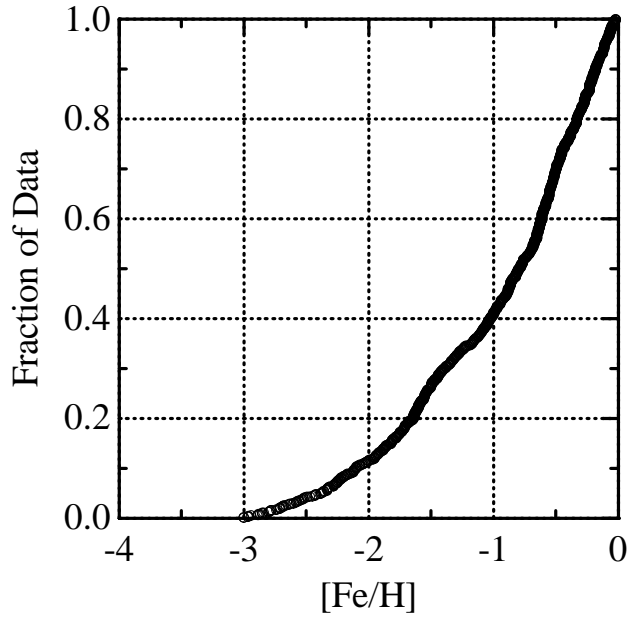
(a) EC Cool Stars



(b) EC Hot Stars



(c) High Proper Motion Stars



(d) HK Survey Stars

